Limnological, Sediment, and Aquatic Macrophyte Biomass Characteristics in Half Moon Lake, Eau Claire, Wisconsin, 2013

Interim Letter Report
10 November, 2014

William F. James
University of Wisconsin – Stout
Sustainability Sciences Institute Discovery Center – 123 E Jarvis Hall
Center for Limnological Research and Rehabilitation
Menomonie, Wisconsin 54751

BACKGROUND AND OBJECTIVES

Management to reduce internal phosphorus (P) loading and algal growth to improve underwater light condition for native aquatic plants has been threefold for Half Moon Lake, Eau Claire, Wisconsin (James et al. 2002). Motor boat activity has been restricted on the lake to reduce P resuspension. Canopy-shading of native macrophytes and P recycling caused by curly-leaf pondweed decomposition were controlled by annual early spring herbicide treatments during the years 2009-2013 to selectively target this species with minimal impact to native plants. Finally, P release from sediments was managed during the year 2011 (application occurred during 15-18 June, 2011) using buffered alum-aluminate to drive algal productivity toward P-limited growth. The goal was to decrease internal P loading from sediment by at least 90% in order to reduce algal biomass and increase light penetration. The objectives of this interim letter report are to describe limnological conditions and aquatic macrophyte response in 2014 to overall lake rehabilitation.

METHODS

Lake Limnological Monitoring

Six stations were established in the lake for water quality monitoring purposes (Figure 1; Table 1). Monitoring was conducted biweekly at each station between May and September, 2014. Water temperature, dissolved oxygen, conductivity, and pH were measured in situ at 0.5-m intervals using a sonde unit (Hydrolab Quanta, Hach Inc., Loveland, CO) that was precalibrated against known standards and Winkler titrations. Secchi disk transparency was measured at each station by lowering a 20-cm diameter alternating black and white disk into the water column until it could not be seen, then slowly pulling it back up until visible, and recording the depth of visibility. Underwater photosynthetically-active radiation (PAR) was measured at 25-cm intervals using a cosine quantum radiometer (Model LI1000, Li-Cor, Inc., Lincoln, NE). The light attenuation coefficient was calculated as,

$$k_d = \frac{\ln(I_o) - \ln(I_z)}{z}$$

where I_o is the surface PAR ($\mu E/cm^2$ s) and I_z is the PAR at depth z (m). In general, k_d is inversely related to Secchi disk transparency. Thus, higher k_d reflects lower light penetration into the water column and a lower Secchi disk transparency.

Water samples integrated over the upper 1 m were collected biweekly for analysis of total P, soluble reactive P, viable chlorophyll, and total alkalinity. Total P samples were predigested with potassium persulfate according to Ameel et al. (1993). Total and soluble reactive P (i.e., P available for uptake by algae) were analyzed colorimetrically using the ascorbic acid method (APHA 2005). Samples for viable chlorophyll (i.e., a surrogate measure of algal biomass) were filtered onto glass fiber filters (Gelman A/E; 2.0 μ nominal pore size) and extracted in 50:50 dimethyl sulfoxide:acetone before fluorometric determination (Welchmeyer 1994). Total alkalinity was determined via titration of unfiltered water samples with 0.02 N sulfuric acid to a pH endpoint of 4.8 according to APHA (2005).

Storm Sewer Monitoring

Automated storm water samplers (ISCO model 6700) and flow loggers equipped with area-velocity sensors (ISCO model 4150) were initially deployed at 4 storm sewers in 2014 to determine phosphorus concentration and loading (Figure 1). Vandalism resulted in destruction of the sampling station at storm sewer 3 (Figure 1). Loggers were programmed to monitor stage and velocity at 5-min intervals. Storm water samplers collected discrete samples at 15-min intervals during precipitation and runoff events. The discrete samples were composited via flow-weighting in the laboratory for determination of total and soluble reactive P.

Sediment Chemistry

Sediment cores were collected at station 10 and 30 in late June, 2014, for determination of sediment P fractions and rates of P release under anaerobic conditions. A core from each station was sectioned at 1- to 2.5-cm intervals for determination of loosely-bound, iron-bound, and aluminum-bound P using methods described in Hieltjes and Lijklema (1980), Psenner and Puckso (1988), and Nürnberg (1988). Additional subsamples were dried at 105 °C to a constant weight and burned at 500 ^{o}C for determination of moisture content, sediment wet and dry bulk density, and organic matter content (Håkanson and Jansson 2002).

Five replicate cores were also collected at each station for determination of P release from sediment under anaerobic conditions. The cores were drained of overlying water and the upper 10 cm of sediment was transferred intact to a smaller acrylic core liner (6.5-cm dia and 20-cm ht) using a core remover tool. Surface water collected from the lake was filtered through a glass fiber filter (Gelman A-E) and 300 mL was siphoned onto the sediment contained in the small acrylic core liner without causing sediment resuspension. Sediment incubation systems were placed in the darkened environmental chamber and incubated at a constant temperature (20 ^{o}C). The oxidation-reduction environment in the overlying water was controlled by gently bubbling nitrogen (anaerobic) through an air stone placed just above the sediment surface in each system.

Water samples for soluble reactive P were collected from the center of each system using an acid-washed syringe and filtered through a 0.45 µm membrane syringe filter (Nalge). The water volume removed from each system during sampling was replaced by addition of filtered lake water preadjusted to the proper oxidation-reduction condition. These volumes were accurately measured for determination of dilution effects. Soluble reactive P was measured colorimetrically using the ascorbic acid method (APHA 2005). Rates of P release from the sediment (mg/m^2 d) were calculated as the linear change in mass in the overlying water divided by time (days) and the area (m^2) of the incubation

core liner. Regression analysis was used to estimate rates over the linear portion of the data.

Aquatic Macrophytes

In June and August, 2014, submersed macrophyte biomass was quantified at ~150 stations in the lake using the point-intercept method (Madsen, 1993). In early May, numbers of germinated curly-leaf pondweed turions per square meter were quantified at each station. A rake-pull method was used to collect samples. The rake was lowered to the sediment and raised to the lake surface at a constant, slow rate while twisting the handle to snag macrophyte stems within a ~ 0.13 m^2 area. The samples were sorted by species and dried to a constant mass at 65 ^oC in a forced-air drying oven. Biomass (g/m^2) at each station was estimated as dry mass divided by the circular area covered by a 180 degree twist of the rake. The rake-pull method provides a reasonably accurate biomass estimate for species such as curly-leaf pondweed and Eurasian watermilfoil that is comparable to diver quadrat sampling (Johnson 2010). However, it overestimates biomass in areas dominated by coontail, elodea, and flat-stemmed pondweed because these species tend to inter-tangle with plants outside the quadrat area, resulting in unintended sampling from an area wider than that of the rake diameter (Johnson 2010). Thus, caution needs to be used when interpreting biomass data dominated by these species.

RESULTS AND DISCUSSION

Sediment characteristics in 2014

Al treatment occurred during the period 15-18 June, 2011. The target dosage goal for the western arm of the lake was 150 g Al/m^2 while the eastern arm and southern (i.e., south of the causeway) embayment target concentration was 75 g Al/m^2. Braun's Bay was not treated with Al.

In 2014, detailed inspection of sediment moisture content and wet bulk density vertical profile characteristics suggested that the Al floc was largely positioned on top of the original sediment interface and had not penetrated appreciably into the sediments three years post-treatment. For cores collected in the western arm of the lake (i.e., station 10) in 2014, sediment wet bulk density was very low, while moisture content approached 95%, in the upper 3-cm layer, contrasting substantially with original surface sediment physical characteristics before the Al treatment (Figure 2). East arm sediments exhibited a similar pattern of lower wet bulk density and higher moisture content over the upper 2-cm layer compared to 2010 conditions (Figure 3). Differences in the apparent thickness of these layers were probably attributed to application of 2X more Al (i.e., 150 g/m^2) in the west versus the east (i.e., 75 g/m^2) arm of the lake. Overall, wet bulk density in the upper 1 cm at both stations declined substantially from ~ 1.04 g/cm^3 in 2010 a mean 1.02 g/cm^3 (±0.003 SE; n = 8), while moisture content increased from 91.5% to a mean 95.6% (± 0.7 SE; n = 8), after Al treatment (Figure 4). These patterns suggested that the bulk density of the consolidated Al floc layer was, in fact, much lower than that of the original sediment surface layer 3 years post treatment.

Prior to Al treatment in 2010, iron-bound P concentrations were greatest in the upper 5-cm sediment layer at both stations. Concentrations within this layer were greatest in west arm, exceeding 1.5 mg/g (Figure 2), versus much lower iron-bound P concentrations in east arm sediments (0.32 mg/g; Figure 3). In 2014, iron-bound P concentrations in west arm sediments were relatively low in the upper 3 cm Al layer and increased substantially at depths below the original 2010 sediment interface, reflecting 2010 concentrations. Iron-bound P was also lower within the upper 2-cm of the original sediment interface in 2014, relative to 2010 concentrations, indicating probable sequestration of some of the iron-bound P immediately below the original sediment interface. In contrast, aluminum-bound P concentrations were maximal in the upper 3-cm layer in conjunction with high Al concentrations. Similar vertical patterns in iron-bound and aluminum-bound P were observed in east arm sediments (Figure 3).

Annual trends in surface sediment iron-bound P suggested that concentrations have been increasing over time since Al treatment primarily for west arm sediment, but not east arm sediments (Figure 5). Iron-bound P in west arm sediments was very low in the Al floc layer (i.e., upper 1 cm) shortly after treatment in 2011, but steadily increased over time to 0.33 mg/g in 2014. This buildup has been approximately linear over time (Figure 6) and may be related to upward diffusion of porewater iron and P into the Al floc from sediments located below the original interface. Between-arm differences in iron-bound P concentrations in the upper 1-cm layer in 2014 were probably related to concentration differences in the original sediment surface layer prior to Al application (Figure 5). The establishment of steep vertical P (and Fe) gradients between original surface sediment and the overlying Al floc in west arm sediments probably drove enhanced upward P diffusion, relative to the east arm where vertical concentration gradients were much lower. While some of this upward P flux was probably sequestered by the Al floc, a portion clearly became re-adsorbed to Fe in west arm sediments with the potential for diffusive flux into the overlying water column under reducing conditions.

Laboratory-derived rates of P release from sediment for west arm sediments under anaerobic conditions increased from undetectable during the first 2 years post-treatment to a mean 1.0 mg/m^2 d (± 0.3 SE; n = 5) by 2014 (Figure 7). While the 2014 anaerobic P release rate represented an ~ 90% decrease from the pretreatment mean of 11.8 mg/m^2 d (±1.7 SE) it, nevertheless, represented a potential source of P to the water column. For east arm sediments, the anaerobic P release rate was essentially undetectable during the 2011-13 post-treatment years and very low at 0.18 mg/m^2 d (± 0.05 SE) in 2014 (Figure 7). Anoxic conditions were detected above the sediment interface at west arm stations 10 and 20 in late June and mid-August, 2014 (Figure 8). East arm stations 30 and 40 exhibited bottom-water anoxia primarily in late August, 2014, only (Figure 8). Thus, potentially reducing conditions conducive for anaerobic P release from sediments were limited in 2014.

Water quality trends after Al treatment

Total P concentrations declined to a minimum at stations 10 through 50 between late May and mid-June (Figure 9), coinciding with similar declines in chlorophyll to very low concentrations (i.e., < 10 µg/L; Figure 10). Secchi transparency extended to the lake bottom during this period (Figure 11) and k_d (i.e., attenuation of PAR) was less than 1 m^{-1} (Figure 12). These patterns were consistent with the suggestion that zooplankton grazing was high, resulting in a late spring clearing phase.

In the deeper western arm of the main basin (i.e., stations 10 and 20), total P concentrations increased rapidly in July and exhibited peaks in August that approached 0.06 mg/L (Figure 9). Chlorophyll followed a similar pattern of rapidly increasing concentrations between mid-June and mid-August in this region of the lake, with maximal concentrations that exceeded 80 µg/L by late August (Figure 10). Secchi transparency declined to less than 1 m during this period (Figure 11); the lowest since Al treatment in 2011. The light attenuation coefficient, k_d, increased to maxima near 3 m^{-1}, indicating severe PAR limitation for summer submersed macrophyte communities (Figure 12).

The eastern arm (stations 30 and 40) of the lake exhibited somewhat seasonally lower total P, chlorophyll, and k_d, and high Secchi transparency, during the height of the phytoplankton growing season compared to the western arm (Figures 9-12). However, prominent peaks in chlorophyll approached or exceeded 60 µg/L by late August with concomitant decreases in Secchi transparency to less than 1 m. In contrast, south embayment (station 50) exhibited relatively low total P and chlorophyll concentrations, Secchi transparency exceeded 1 m, and PAR attenuation was lower during the late August bloom, despite constant total P and soluble P loading into the embayment via the Owen Park shallow groundwater pumps (*see below*).

Trends at station 60 (i.e., Braun's Bay) contrasted sharply from those observed in the main basin of the lake. Total P concentrations steadily decline from ~ 0.035 mg/L in May

and June to less than 0.020 mg/L in September (Figure 9). Chlorophyll concentrations were very low, usually less than 10 μg/L (Figure 10), Secchi disk transparency extended to the lake bottom (Figure 11), and PAR attenuation was less than 1 m^{-1} (Figure 12) throughout the summer, indicating good solar radiation penetration down to the lake bottom for submersed aquatic macrophyte growth.

Overall trends in July-September mean total P, chlorophyll, and Secchi transparency in the main basin (i.e., stations 10-40) are shown in Figure 13. The period July-September was chosen because it represented the typical period of maximum nuisance algal blooms and did not include the late May-June clearing phase caused by zooplankton grazing. Mean total P and chlorophyll increased, while Secchi transparency declined, in 2014 relative to other post-treatment years. In particular, the mean chlorophyll concentration for 2014 approached means observed in 2008 and 2010, before Al treatment. In addition, the main basin mean chlorophyll concentration was unusually high compared to mean total P and Secchi transparency in 2014 (Table 2 and 3). While the Carlson TSI_{TP} and TSI_{SD} were similar at ~ 59-61, TSI_{CHLa} was much higher at 68 (Table 3). The relatively high mean CHLa:TP of ~1.07:1 indicated that chlorophyll production was near maximal within the range of total P concentrations and may reflect dominance by a specific group or taxa of cyanobacteria (Jones et al. 2011). Phytoplankton enumeration is currently underway to evaluate community dynamics during 2014. Trends in mean summer total P, chlorophyll, and Secchi transparency for various areas of the lake indicated that impairment was greatest in the west arm while south embayment variables reflected continued improved water quality conditions post-treatment (Figure 14).

Predicted maximum inhabitable depth for stem- and rosette-forming submersed macrophytes, based on the percentage of surface PAR radiation penetrating the water column (Middelboe and Markager 1997), declined in 2014 (Figure 15). Underwater PAR habitat impairment was greatest in the west arm (Figure 16), reflecting lower native biomass in 2014 compared to other years (see below). The predicted maximum inhabitable depth declined by ~ 0.4 m to 2.6 m for stem-forming submersed macrophytes and by 0.2 m to 1.1 m for rosette- and meadow-forming submersed macrophytes.

Post herbicide treatment trends in curly-leaf pondweed and native submersed vegetation

2013 represented the fifth consecutive year of endothall treatment to reduce the curly-leaf pondweed turion bank in the sediment. Point-intercept sampling for germinated turions occurred at the end of April, 2014, due to a late spring and ice-off in late April. The winter of 2013-14 was unusually cold with significant snowfall accumulation on the lake ice that probably suppressed PAR penetration and submersed macrophyte growth. Turion germination was very low (Figure 17) in April, 2014, suggesting that the turion bank had been significantly depleted after 5 years of treatment. The frequency of occurrence was only 18%. Based on these findings, a sixth consecutive early spring herbicide treatment was not conducted.

Surprisingly, CLP growth rebounded after herbicide treatment cessation and was present at over 40% of the point-intercept locations by June, 2014 (Figure 18). June biomass also rebounded substantially from other treatment years to a lakewide average of 20 g/m^2 (Figure 17). Discrepancies in CLP frequency between April and June, 2014, suggested that significant turion germination occurred in May that was not captured by the late April sampling event. Current conceptual models suggest that turion germination occurs primarily during fall and under winter ice cover (Figure 19). However, CLP population dynamics in Half Moon Lake did not appear to fit this general germination pattern. Rather, germination timing may be much more complex and regulated by factors such as snow and ice cover, winter PAR penetration, the timing of ice-out, and spring temperature patterns. Indeed, significant turion germination may occur in May regardless of annual variations in winter and early spring conditions and needs to be considered in CLP control.

Native submersed macrophyte biomass was again dominated by Elodea in 2014; some other native species were also observed (Stargrass, wild celery, coontail). Although native biomass frequency of occurrence was greater than 80% in both June and August

2014, biomass declined substantially in August over previous years (Figure 20). Biomass declines were greatest in the deeper west arm of the lake (not shown). This pattern was probably related, in large part, to lower Secchi transparency and higher k_d in 2014.

Storm sewer hydrology and phosphorus inputs to Half Moon Lake

During the summer period, monthly rainfall was above normal in June and August through September, 2014 (Figure 21). Storm frequency and intensity were also high throughout the summer, with greater than 1 inch of rainfall occurring on several occasions (Figure 22). A minor dry period occurred in July and late September only. Overall, precipitation in 2014 was well above the ~20 inch average for the May-September period at ~ 28 inches. Pool elevation exceeded the nominal 769.8 ft MSL throughout the May-September period as a result of frequent storm runoff and inputs from the Owen Park shallow groundwater pumps (Figure 23).

Approximately 85 storm-related or base flow events were collectively captured at storm sewers 1, 2, and 4 for determination of total and soluble reactive P concentrations in 2014. Unfortunately, the equipment box located at storm sewer 3 was vandalized, removed from the site, and latter found in the lake. Flow increased at all monitored storm sewers as a result of storms (Figure 24-26). At storm sewer 1, shallow groundwater pumps (up to 3 pumps) provided a continuous base flow of Chippewa River groundwater to Half Moon Lake (Figure 24). Three pumps were operational between mid-June and the end of August, providing a base flow of ~ 3.0 ft^3/s (Figure 24).

Mean summer (i.e., June-September) storm flow at station 2 and 4 more than doubled in 2014 compared to other years in conjunction with greater precipitation (Figure 27 and Table 4). However, storm flow at station 1 was not unusually high and did not reflect greater precipitation in 2014. Mean base flow at storm sewer 1 was slightly lower in 2014 versus 2013 and other years due to differences in pump output between years. Measured mean storm flow was also greatest at sewer 1 at 0.158 ft^3/s, followed by sewer 2 at 0.090

ft^3/s, and sewer 4 at 0.023 ft^3/s (Table 4). Summer flow at storm sewers 2 and 4 was equivalent to ~ 4% and 1% of the summer flow at storm sewer 1.

The measured mean storm flow-weighted total P concentration was greatest for storm sewer 1 at 0.295 mg/L (Figure 28 and Table 5). This mean, however, was lower compared to other years. Base-flow total P at storm sewer 1 was 0.084 mg/L, which was slightly lower but comparable to base-flow concentrations during other years. Mean total P was moderately high at 0.102 and 0.171 mg/L for storm sewers 2 and 4, respectively, in 2014 and comparable to mean concentrations during other years. Mean storm flow soluble reactive P concentrations ranged between 0.026 mg/L (i.e., storm sewer 2) and 0.045 mg/L (i.e., storm sewers 1 and 4). In general, event mean SRP concentrations were slightly elevated in 2014 compared to 2012 and 2013.

As in previous years, storm sewer 1 dominated measured total and soluble reactive P loading in 2014 (Figure 29 and Tables 6 and 7). However, P loading from this storm sewer was lower in 2014 compared to 2013 due to slightly lower base flow and event mean P concentrations in 2014. Over the June-September summer period, storm sewer 1 discharged ~ 70 kg total P and 30 kg SRP. Storm sewer 1 base flow contributed most of the SRP loading, which represented 42% of the base flow total P loading. By comparison, SRP loading accounted for only 5% of the storm flow total P load at this site. Storm sewer 2, which drained a much smaller subwatershed, contributed only ~3.4 kg total P over the summer period. However, SRP accounted for ~ 50% of this load. Storm sewer 4, which received drainage from the Carson Park stadium parking lot that discharges into Braun's Bay, contributed ~ 1.4 kg total P over the summer. SRP represented only 18% of the total P load from this site.

Analysis of phosphorus sources and fluxes

Given that both P and chlorophyll concentrations increased markedly in Half Moon Lake during the summer period of 2014 (Figure 30), P mass fluxes were estimated for various regions in the lake for comparison with measured P fluxes from the sediment and

the Owen Park input. The goal of this analysis was to infer potential roles that some of the major external and internal P sources may be playing in driving the development of algal blooms in 2014. Net rates of P mass accumulation in the lake increased linearly during the period mid-June through late July (i.e., 41 day period) both lakewide (excluding Braun's Bay) and in various regions (i.e., west arm, east arm, south arm; Figure 31). Net P mass accumulation rates during this period were greatest in the west arm at 1.7 mg/m^2 d and lowest in the south arm at 0.7 mg/m^2 d (Table 8). The estimated lakewide net P mass accumulation rate was 1.3 mg/m^2 d (Table 8).

Although P mass balance was difficult to quantify, comparisons provided some important insights into possible causes for the extensive algal blooms in the lake in 2014. Although P inputs from the Owen Park pumps were ~ 24 kg during the 41 day period, net P mass accumulation in the south arm of the lake, which receives these inputs, was only 3 kg (Table 8). This P input was probably largely short-circuiting into the Becca Brook outlet, located in the embayment south of the storm sewer, rather than moving into the main arm. Because bottom water anoxia was not detected in the south arm of the lake, I estimated zero anaerobic P release from sediments in this region. Lateral transport of P from the south to the east arm could not be estimated.

Net P mass accumulation was greatest in the west arm at ~20 kg versus only 7 kg in the east arm (Table 8). Although the anaerobic P release rate was ~ 1 mg/m^2 d for sediments located in the west arm, bottom water anoxic conditions were documented only in late June in both east and west arms (Figure 8). Assuming an anoxic period of 7 days, west and east arm sediments could have released ~ 2 and 0.2 kg, respectively, during the 41-day period. Thus, possible anaerobic P release from sediments would not explain the much greater net P mass accumulation rates in the water column of the west and east basins.

While preliminary (phytoplankton enumeration is currently in progress and forthcoming), excystment of cyanobacterial resting spores residing in the sediment and inoculation of the water column may provide the most plausible working hypothesis to

explain 2014 summer chlorophyll patterns. Similarly, an algal bloom composed primarily of the cyanobacterial species, *Cylindrospermopsis*, developed in the west arm of the lake in August, 2011, after the Al application. This pattern was attributable to a couple of factors that resulted in its unexpected success. This species overwinters as a spore or cyst in the sediment and probably assimilated luxury P (i.e., P stored in cells as polyphosphates well in excess of growth requirements) from the sediment well before the Al treatment occurred. These reserves were used in bloom development after excystment, providing the population with a competitive advantage over other species that did not scavenge P before the Al treatment.

Bloom suppression in 2012 and 2013 could have been linked to low mobile P concentrations (i.e., iron-bound P) in the sediment as well as negligible anaerobic diffusive P flux from sediment into the overlying water column due to the Al treatment. *Cylindrospermopsis* sp were detected in August and September of both years, but in low concentration. Higher mobile P concentrations in sediment in 2014, particularly in west arm sediments, may have played a role in subsidizing direct P uptake and assimilation by *Cylindrospermopsis* spores or another species with a similar life history of resting stages in the sediment. Thus, although sediment mobile P concentrations and anaerobic P release rates were still low in 2014 relative to pretreatment conditions, direct uptake of this new P source, that diffused upward from deeper sediment layers, by cyanobacterial spores, excystment, and water column inoculation would provide a plausible mechanism explaining chlorophyll bloom formation in 2014.

MANAGEMENT RECOMMENDATIONS

Curly-leaf pondweed

It is apparent that the turion bank in Half Moon Lake sediments is still viable after 5 years of early spring endothall treatments. Future CLP control measures should consider additional endothall treatments on an annual basis. However, the number of treatment years required to reduce the turion bank remains unknown. Other studies have reported

some CLP suppression after up to 7 years of herbicide control (Johnson et al 2012). Research findings on longer-term treatment programs have not been published. However, additional management via early spring endothall treatments may be required for several years. Alternatively, the harvesting program could be re-established.

Quantifying turion germination has become more problematic in light of recent findings. It appears that turion germination is very significant in April and May. Ideally, seasonal germination patterns should be examined in order to better understand and predict the optimal timing for treatment. A caveat has been that treatments have generally occurred in late April in conjunction with a water temperature range of 15 to 18 C to maximize selective control of CLP. While April point-intercept sampling has generally shown a declining germination trend over time, this approach has failed to account for projected later germination. Additionally, herbicide applications have probably inadvertently controlled these later germinations, as indicated by frequency and biomass trends in June. Germinated turion assessment should probably continue although perhaps in later spring to more accurately quantify frequency of germinated turions. Ultimately, depletion of the turion bank can best be assessed by evaluating frequency and biomass during a nontreatment year.

Algal blooms and PAR attenuation

The native macrophyte community is clearly being impacted by high PAR attenuation, particularly in the west arm of the lake, due to the reemergence of cyanobacterial blooms in 2014. The current working hypothesis suggests that porewater Fe and P have slowly diffused from deeper sediment layers into the surface Al floc layer over time. While the Al floc may be sequestering some of this P, another portion is now coupled with Fe and can diffuse into the overlying water column under reducing conditions. More importantly, this P is directly available for uptake by cyanobacterial spores residing in the sediment of Half Moon Lake (i.e., working hypothesis). Even though an adequate Al dosage was applied to inactivate the high sediment mobile P concentrations, the Al floc did not sink into the upper sediment due to higher bulk density characteristics of the

original sediment interface. Thus, Al binding efficiency has probably decreased over time (de Vicente et al. 2008a and b), allowing for upward P diffusion through the Al floc and re-adsorption onto Fe~(OOH) (Lewendowski et al. 2003). This outcome is most apparent in west arm sediments, where mobile P concentrations were extraordinarily high in the original surface sediment layer. Although similar diffusional processes are occurring in east arm sediments, much less mobile P has accumulated in the surface Al floc layer due to lower mobile P concentrations in the original surface sediment layer.

Interestingly, sediment P availability for algal bloom development is most likely via direct assimilation by cyanobacterial spores residing in the sediment rather than indirect diffusive P flux into the overlying water column. Reducing conditions that would drive anaerobic P flux were rarely observed above the sediment interface in 2014. Nevertheless, sediment mobile P that has accumulated in the Al floc layer is apparently stimulating cyanobacterial blooms through directly availability in the sediment.

Because mobile P concentrations were so high in the original sediment column and the Al floc could not sink into the sediment to sequester this P, upward P diffusion is likely to continue, reducing Al treatment success and longevity in Half Moon Lake. Thus, long-term Al management (i.e., over several years to decades) may be required that involves applications every two to three years. Al dosage could target binding mobile P in the current Al floc layer (i.e., the upper 3 cm in the west arm and the upper 2 cm in the east arm). Because bulk densities are lower in these layers, addition of a new Al floc has a greater probability of sinking through these surface layers to bind mobile P. De Vicente et al. (2008b) similarly suggested that smaller Al doses spread out over several years might maintain higher P binding efficiencies.

REFERENCES:

Ameel, J.J., Axler, R.P., and Owen, C.J. 1993. Persulfate digestion for determination of total nitrogen and phosphorus in low nutrient water. American Environmental Laboratory (October, 1993):8-10.

American Public Health Association. 2005. Standard methods for the examination of water and wastewater. 21th ed., Washington, DC.

Carlson, R.E. 1977. A trophic state index for lakes. Limnol. Oceanogr. 22:361-369.

de Vicente I, Jensen HS, Andersen FØ. 2008a. Factors affecting phosphate adsorption to aluminum in lake water: Implications for lake restoration. Sci Total Environ 389:29-36.

de Vicente I, Huang P, Andersen FØ, Jensen HS. 2008b. Phosphate adsorption by fresh and aged aluminum hydroxide. Consequences for lake restoration. Environ Sci Technol 42:6650-6655.

Håkanson L, Jansson M. 2002. Principles of lake sedimentology. The Blackburn Press, Caldwell, NJ USA.

Hjieltjes AH, Lijklema L. 1980. Fractionation of inorganic phosphorus in calcareous sediments. J. Environ. Qual. 8: 130-132.

Johnson, J.A. 2010. Evaluation of lake-wide, early-season herbicide treatments for controlling invasive curlyleaf pondweed (*Potamogeton crispus*) in Minnesota Lakes. Master's thesis, University of Minnesota.

Johnson JA, Jones AR, Newman RM. 2012. Evaluation of lakewide, early season herbicide treatments for controlling invasive curlyleaf pondweed (*Potamogeton crispus*) in Minnesota Lakes. Lake Reserv Manage 28:346-363.

Jones JR, Obrecht DV, Thorpe AR. 2011. Chlorophyll maxima and chlorophyll:total phosphorus ratios in Missouri reservoirs. Lake Reserv Manage 27:321-328.

Lewandowski J, Schauser I, Hupfer M. 2003. Long term effects of phosphorus precipitations with alum in hypereutrophic Lake Süsser See (Germany). Wat Res 37:3194-3204.

Madsen, J.D. 1993. Biomass techniques for monitoring and assessing control of aquatic vegetation. Lake Reserv. Manage. 7:141-154.

Middelboe, A.L., and Markager, S. 1997. Depth limits and minimum light requirements of freshwater macrophytes. Freshwat. Biol. 37:553-568.

Nürnberg GK. 1988. Prediction of phosphorus release rates from total and reductant-soluble phosphorus in anoxic lake sediments. Can J Fish Aquat Sci 45:453-462.

Psenner R, Puckso R. 1988. Phosphorus fractionation: Advantages and limits of the method for the study of sediment P origins and interactions. Arch Hydrobiol Biel Erg Limnol 30:43-59.

Welschmeyer, N.A. 1994. Fluorometric analysis of chlorophyll a in the presence of chlorophyll b and pheopigments. Limnol. Oceanogr. 39:1985-1992.

Woolf TE, Madsen JD. 2003. Seasonal biomass and carbohydrate allocation patterns in southern Minnesota curlyleaf pondweed populations. J Aquat Plant Manage 41:113-118.

Table 1. Typical water column depths at the various water sampling stations in Half Moon Lake, Wisconsin.

Station	Nominal Depth	
	(m)	(ft)
10	3.0	9.8
20	3.0	9.8
30	2.5	8.2
40	2.5	8.2
50	2.2	7.2
60	1.8	5.9

Table 2. Mean summer (Jul-Sep) post-alum treatment concentrations of total phosphorus (P), viable chlorophyll (CHLA), Secchi disk transparency, and the light attenuation coefficient (k_d) at various stations in Half Moon Lake in 2014. Main arm = combined west and east arm.

	2014			
Station	Total P (mg/L)	CHLA (ug/L)	Secchi (m)	PAR (m^{-1})
10	0.043	49.9	0.9	1.8
20	0.047	50.0	1.0	1.8
30	0.043	44.3	0.9	1.7
40	0.041	42.8	0.9	1.7
50	0.028	17.3	1.5	1.2
60	0.021	8.3	1.9	0.9
Main arm	0.044	46.7	0.9	1.8

Table 3. Trophic State Index (TSI; Carlson 1977) values derived from mean total phosphorus (TP), viable chlorophyll (chla), and Secchi disk (SD) transparency for the post-alum treatment period (Jul-Sep) of 2014. Main arm = combined west and east arm.

	2014		
Station	TSI_{TP}	TSI_{chla}	TSI_{sd}
10	58.5	68.9	61.1
20	59.7	68.9	60.6
30	58.4	67.8	61.1
40	57.6	67.4	60.8
50	52.4	58.6	53.7
60	48.2	51.4	50.5
Main arm	58.6	68.3	60.9

Table 4. Comparison of mean summer flow in 1999 versus 2012-14 for various storm sewers draining into Half Moon Lake.

Sewer	Location		1999			2012			2013			2014		
			Precip	Flow		Precip	Flow		Precip	Flow		Precip	Flow	
			(inches)	(ft^3/s)	(m^3/s)	(inches)	(ft^3/s)	(m^3/s)	(inches)	(ft^3/s)	(m^3/s)	(inches)	(ft^3/s)	(m^3/s)
1	Owen Park Pumps	Total	9.6	1.220	0.0346	8.3	1.242	0.0352	9.3	2.898	0.0821	23.8	2.454	0.0695
		Storm Flow		0.048	0.0014		0.182	0.0052		0.157	0.0044		0.158	0.0045
		Base Flow		1.172	0.0332		1.058	0.0300		2.742	0.0777		2.296	0.0650
2	Near Midlefort Clinic			0.091	0.0026		0.022	0.0006		0.020	0.0006		0.090	0.0026
3	West of Beach			0.038	0.0011		0.046	0.0013		0.219	0.0062			
4	Carson Park						0.003	0.0001		0.007	0.0002		0.023	0.0006

Table 5. Summer flow-weighted total phosphorus (P) and soluble reactive P (SRP) for various storm sewers in 1999 and 2012-14.

Sewer	Description	1999		2012		2013		2014	
		Total P	SRP	Total P	SRP	Total P	SRP	Total P	SRP
		(mg/L)		(mg/L)		(mg/L)		(mg/L)	
1	Storm Flow	0.344	0.038	0.358	0.019	0.417	0.015	0.295	0.024
1	Base Flow	0.074	0.010	0.109	0.040	0.108	0.043	0.084	0.045
2	Storm Flow	0.149	0.044	0.096	0.011	0.098	0.022	0.102	0.026
3	Storm Flow	0.301	0.045	0.205	0.022	0.204	0.015		
4	Storm Flow					0.178	0.031	0.171	0.042

Table 6. Mean summer (JUN-SEP) total phosphorus (P) and soluble reactive P (SRP) loading for various storm sewers in 1999 and 2012-14.

Sewer	Description	1999		2012		2013		2014	
		Total P	SRP	Total P	SRP	Total P	SRP	Total P	SRP
		(kg/d)		(kg/d)		(kg/d)		(kg/d)	
1	Storm Flow	0.040	0.004	0.159	0.008	0.159	0.006	0.115	0.006
1	Base Flow	0.212	0.029	0.282	0.104	0.725	0.289	0.472	0.241
2	Storm Flow	0.033	0.010	0.005	0.001	0.005	0.001	0.023	0.005
3	Storm Flow	0.028	0.004	0.023	0.002	0.109	0.008		
4	Storm Flow					0.003	0.001	0.009	0.002

Table 7. Summer (JUN-SEP) mass loading of total phosphorus (P) and soluble reactive P (SRP) for various storm sewers in 1999 and 2012-14.

Sewer	Description	1999		2012		2013		2014	
		Total P	SRP	Total P	SRP	Total P	SRP	Total P	SRP
		(kg/summer)		(kg/summer)		(kg/summer)		(kg/summer)	
1	Storm Flow	4.89	0.54	19.29	1.02	19.18	0.69	13.88	0.71
1	Base Flow	25.67	3.47	34.14	12.53	87.73	34.93	57.08	29.22
2	Storm Flow	4.03	1.19	0.63	0.07	0.61	0.14	2.77	0.60
3	Storm Flow	3.43	0.51	2.77	0.30	13.22	0.97		
4	Storm Flow					0.37	0.06	1.07	0.19

Table 8. A comparison of net changes in phosphorus (P) mass in various regions of the lake between mid-June and late July (see Figure 31) versus estimated P fluxes from the Owen Park pumps and anaerobic sediment. Anaerobic sediment P flux, determined from sediment core incubations, was weighted with respect to an anoxic period of ~ 7 days for the west and east arms. P flux in the south arm was assumed to be negligible due to the occurrence of oxic conditions above the sediment interface throughout the summer.

Variable		(mg/m^2 d)	(kg)
Lake net change in P mass	Lake-wide	1.28	30
	West arm	1.68	20
	East arm	1.04	7
	South arm	0.65	3
Owen park pumps[1]		1.04	24
Anaerobic sediment P flux[2]	Lake-wide	0.72	2.3
	West arm	1.04	2.1
	East arm	0.16	0.2
	South arm	0.00	0

[1]JUN-SEP average

[2]Assumes that bottom waters were anoxic for a 7 days during the period of net lake P mass increase

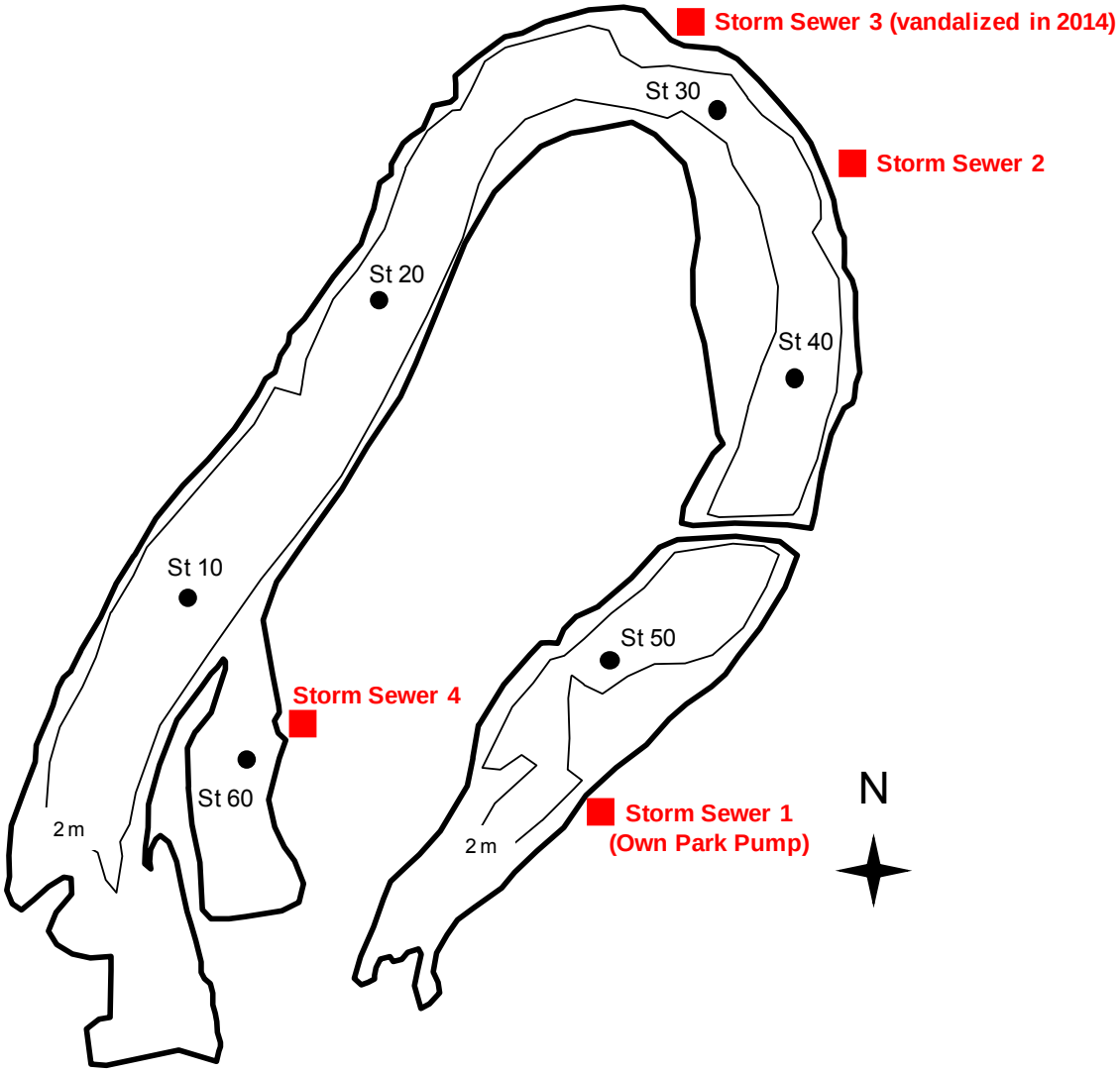

Figure 1. *Sampling station locations in Half Moon Lake.*

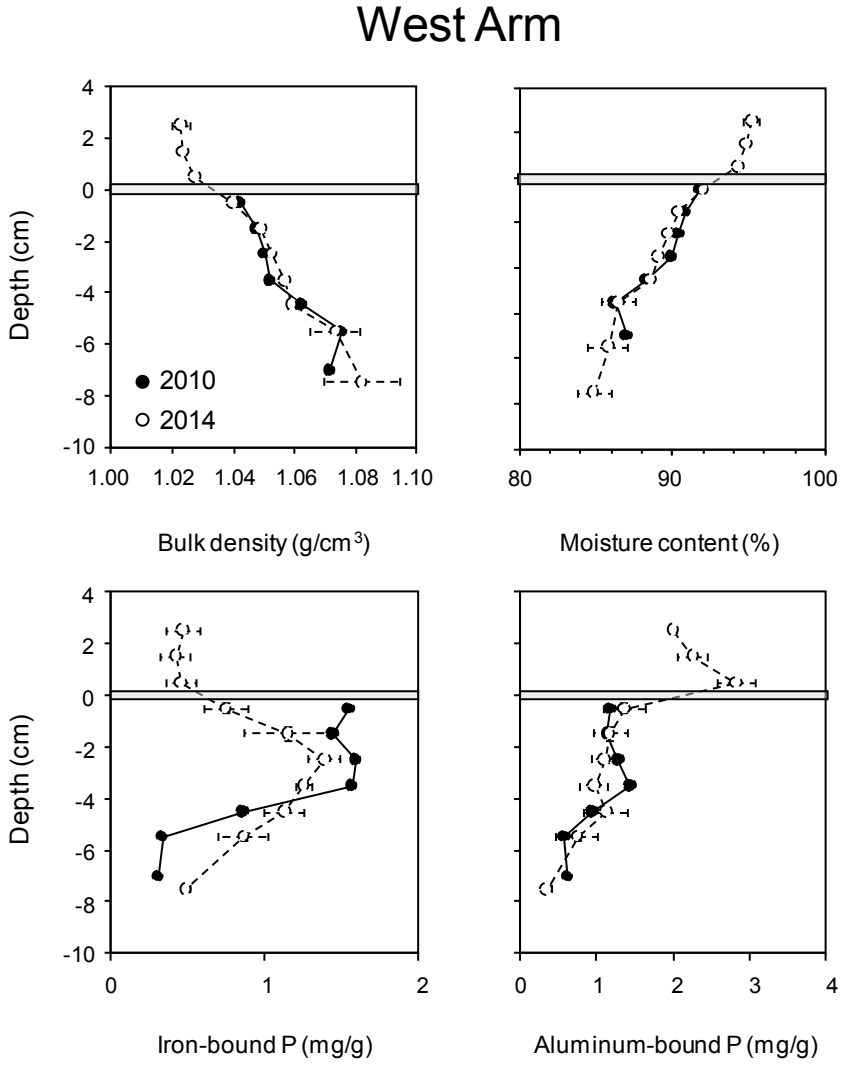

Figure 2. *Variations in sediment wet bulk density (upper left), moisture content (upper right), sediment iron-bound phosphorus (lower left), and aluminum-bound P (lower right) as a function of depth below the sediment-water interface for sediment cores collected at station 10 located in the west arm of Half Moon Lake. The year 2010 represents concentrations before alum treatment and the year 2014 represents conditions in July, three years after Al application. The horizontal gray line denotes the location of the original pretreatment surface sediment-water interface.*

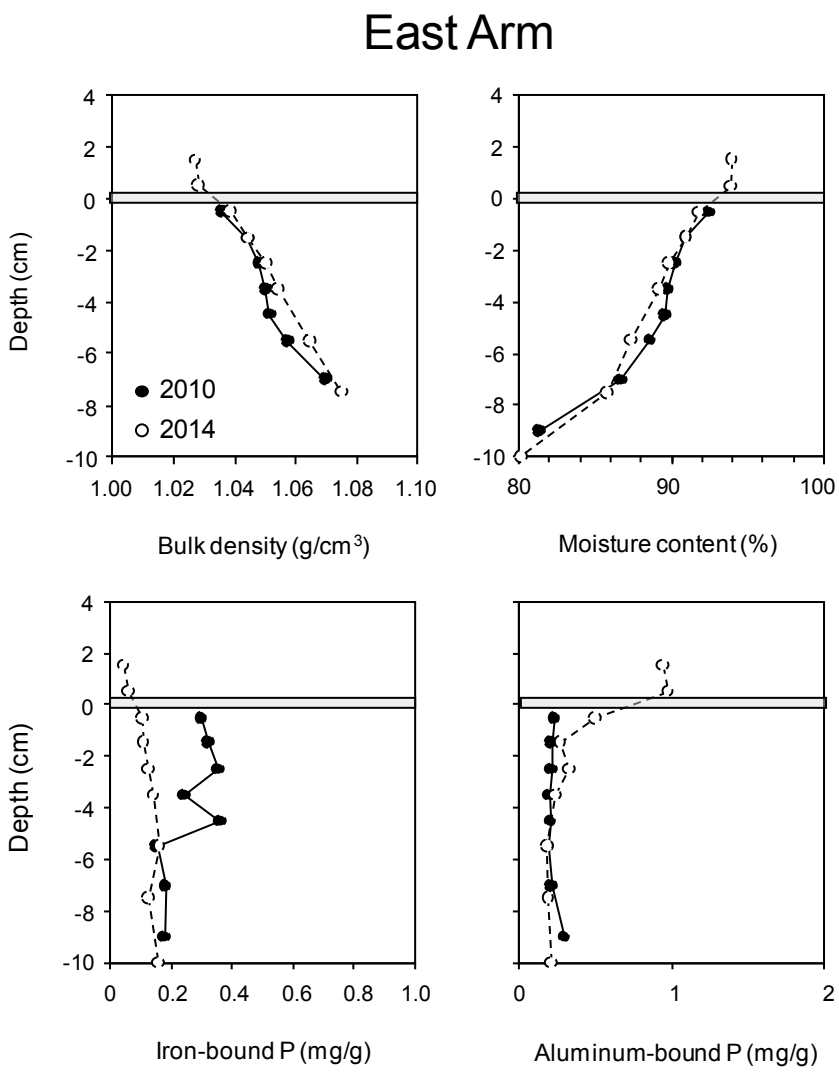

Figure 3. *Variations in wet bulk density (upper left), moisture content (upper right), iron-bound phosphorus (lower left), and aluminum-bound P (lower right) as a function of depth below the sediment-water interface for cores collected at station 30 located in the east arm of Half Moon Lake. The year 2010 represents concentrations before alum treatment and the year 2014 represents conditions in July, three years after Al application. The horizontal gray line denotes the location of the original pretreatment surface sediment-water interface.*

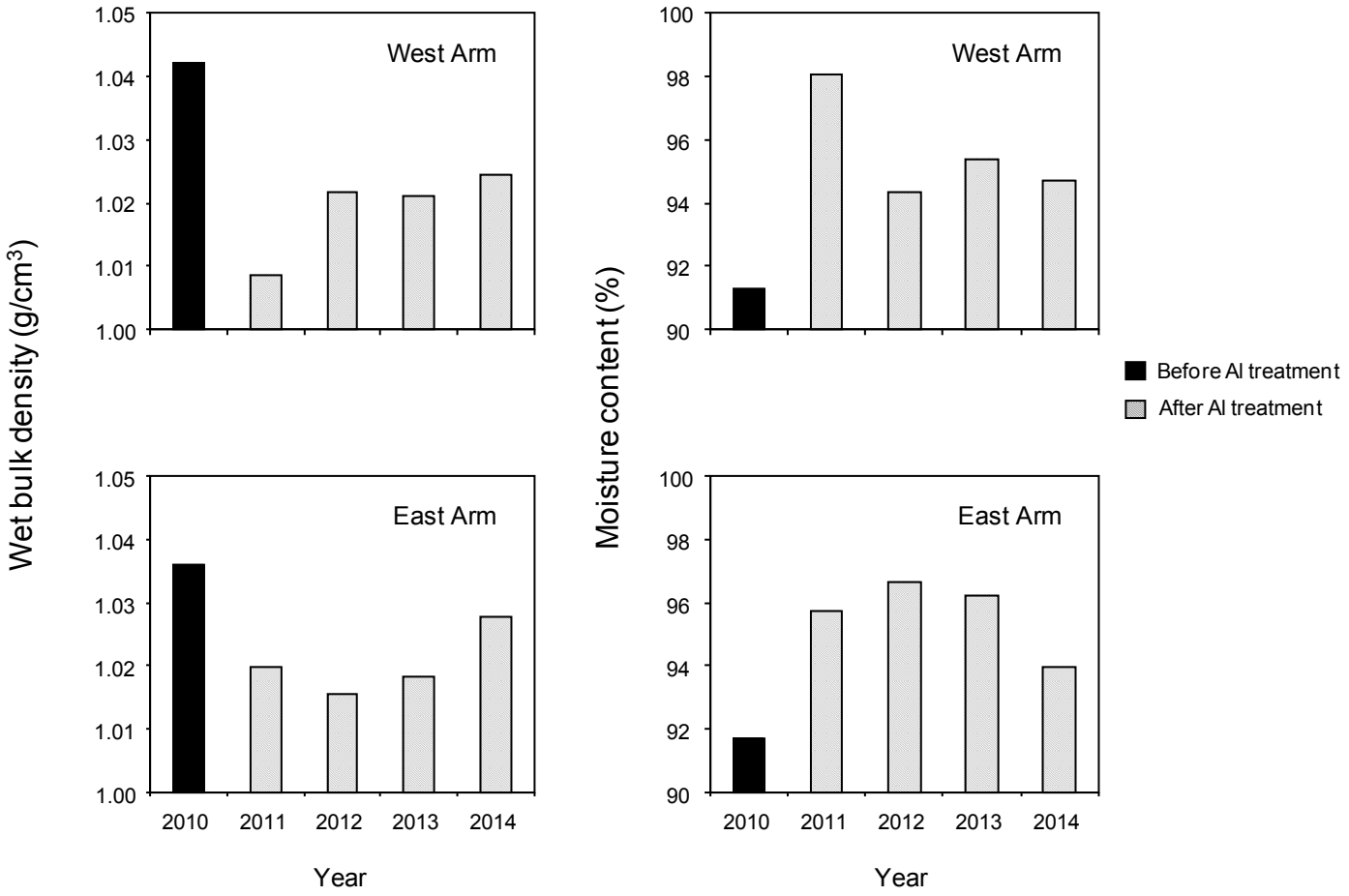

Figure 4. *Annual variations in wet bulk density (left panels) and moisture content (right panels) in the surface (upper 1 cm) sediment layer before and after Al treatment.*

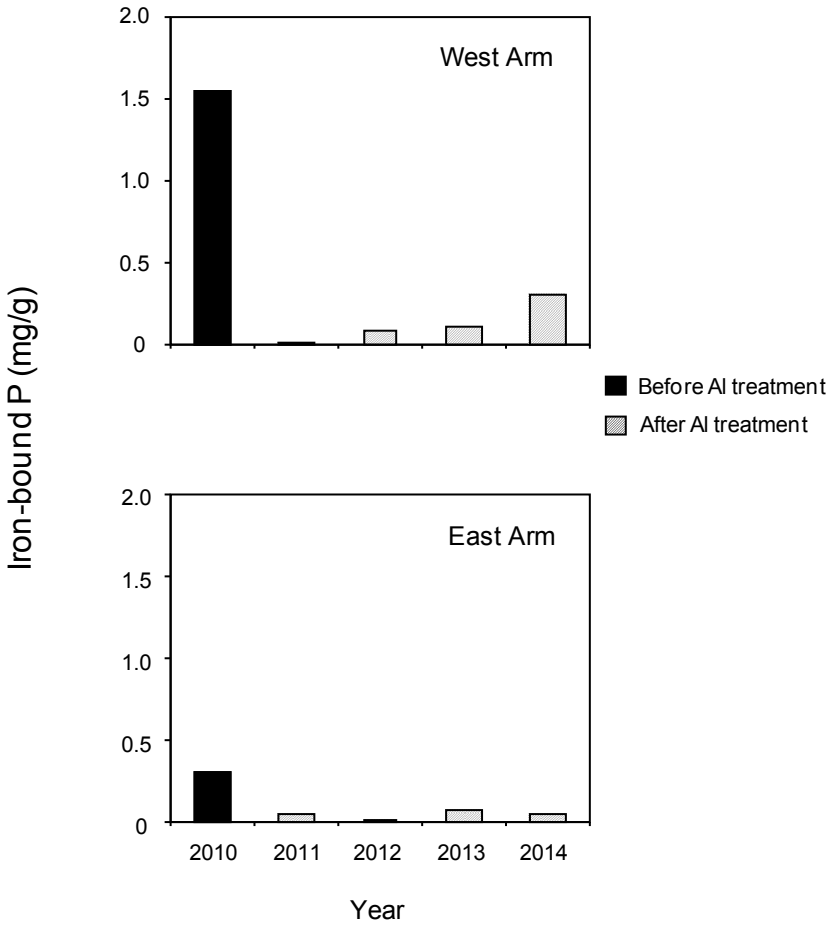

Figure 5. *Annual variations in iron-bound phosphorus (P) in the surface (upper 1 cm) sediment layer before and after Al treatment.*

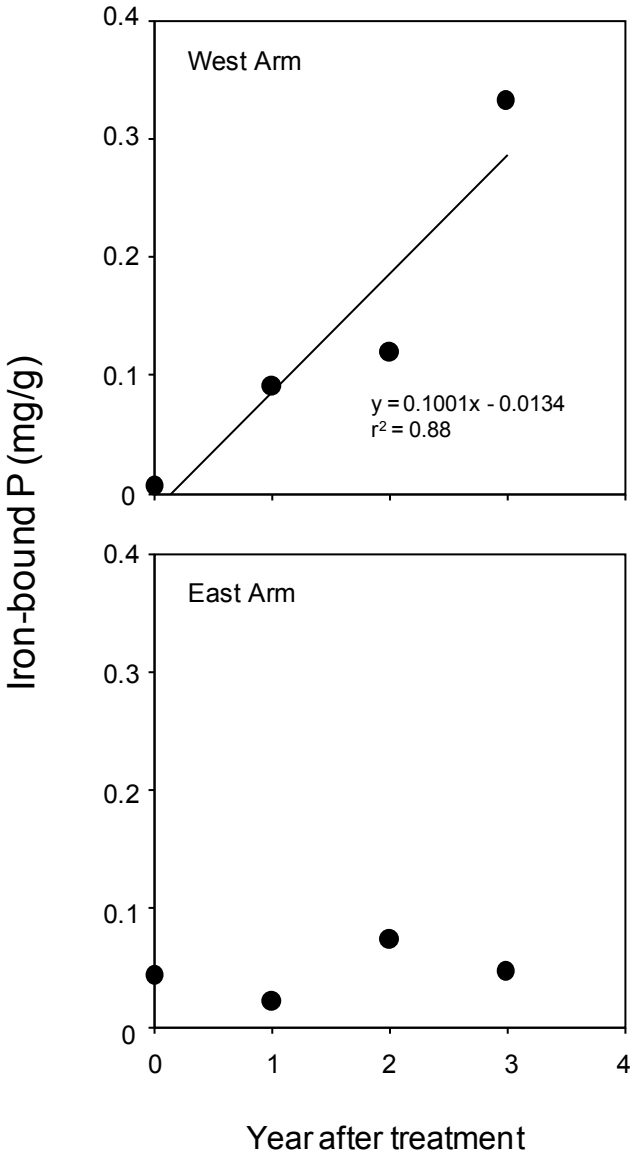

Figure 6. *Relationships between year after Al treatment and the concentration of iron-bound phosphorus (P) in the surface (upper 1 cm) sediment layer.*

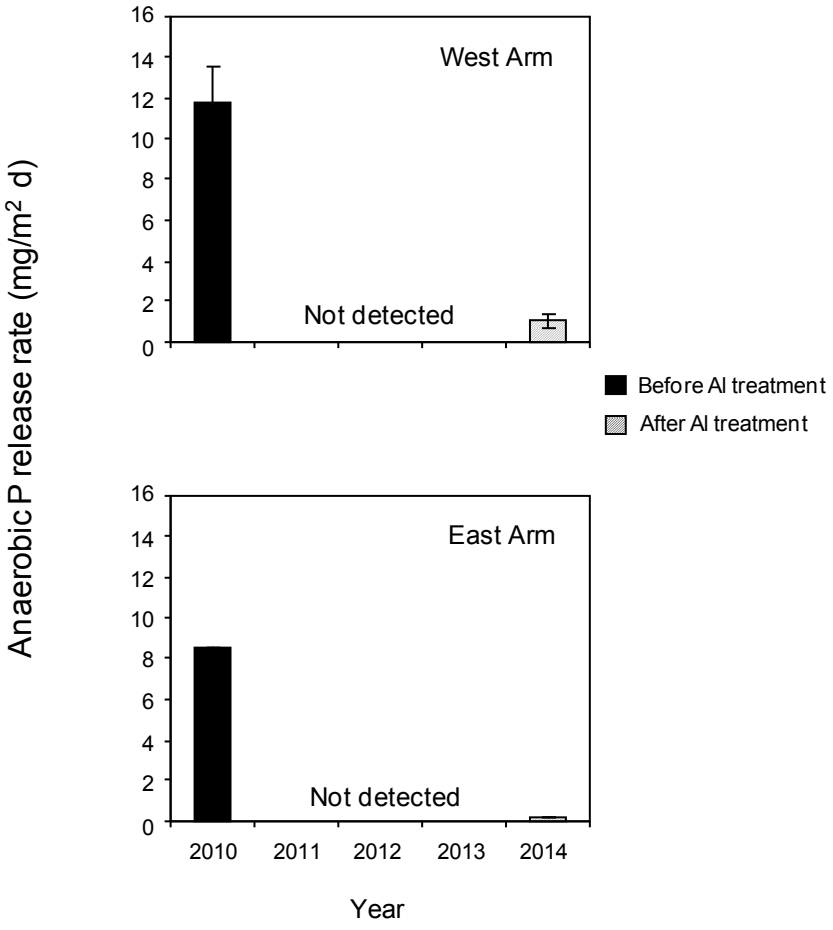

Figure 7. *Annual variations in the mean (n = 5) anaerobic phosphorus (P) release rate before and after Al treatment. Horizontal lines represent 1 standard error.*

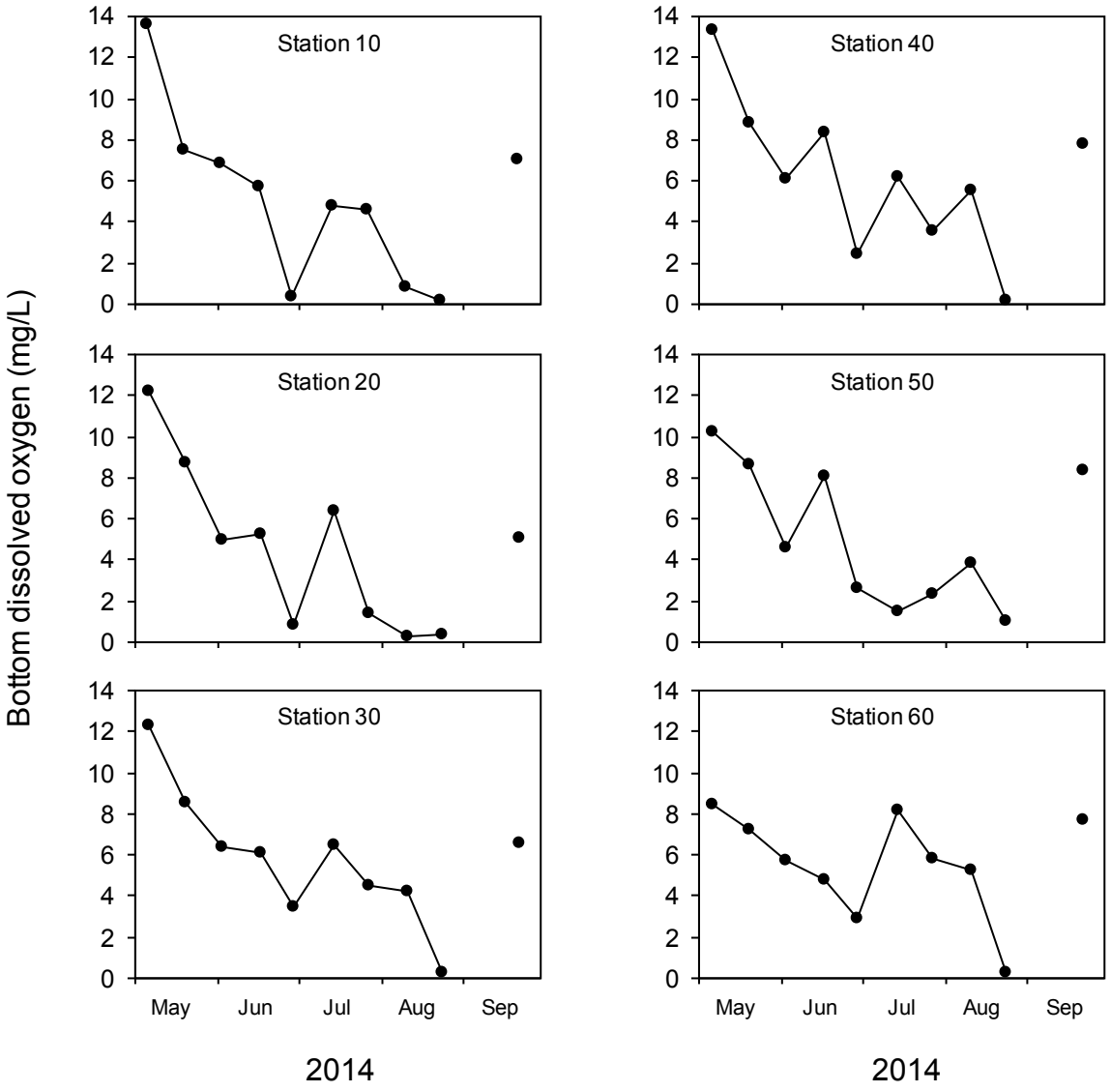

Figure 8. *Seasonal variations in bottom (i.e., ~ 0.25 m above the sediment) dissolved oxygen concentration at various stations in Half Moon Lake in 2014.*

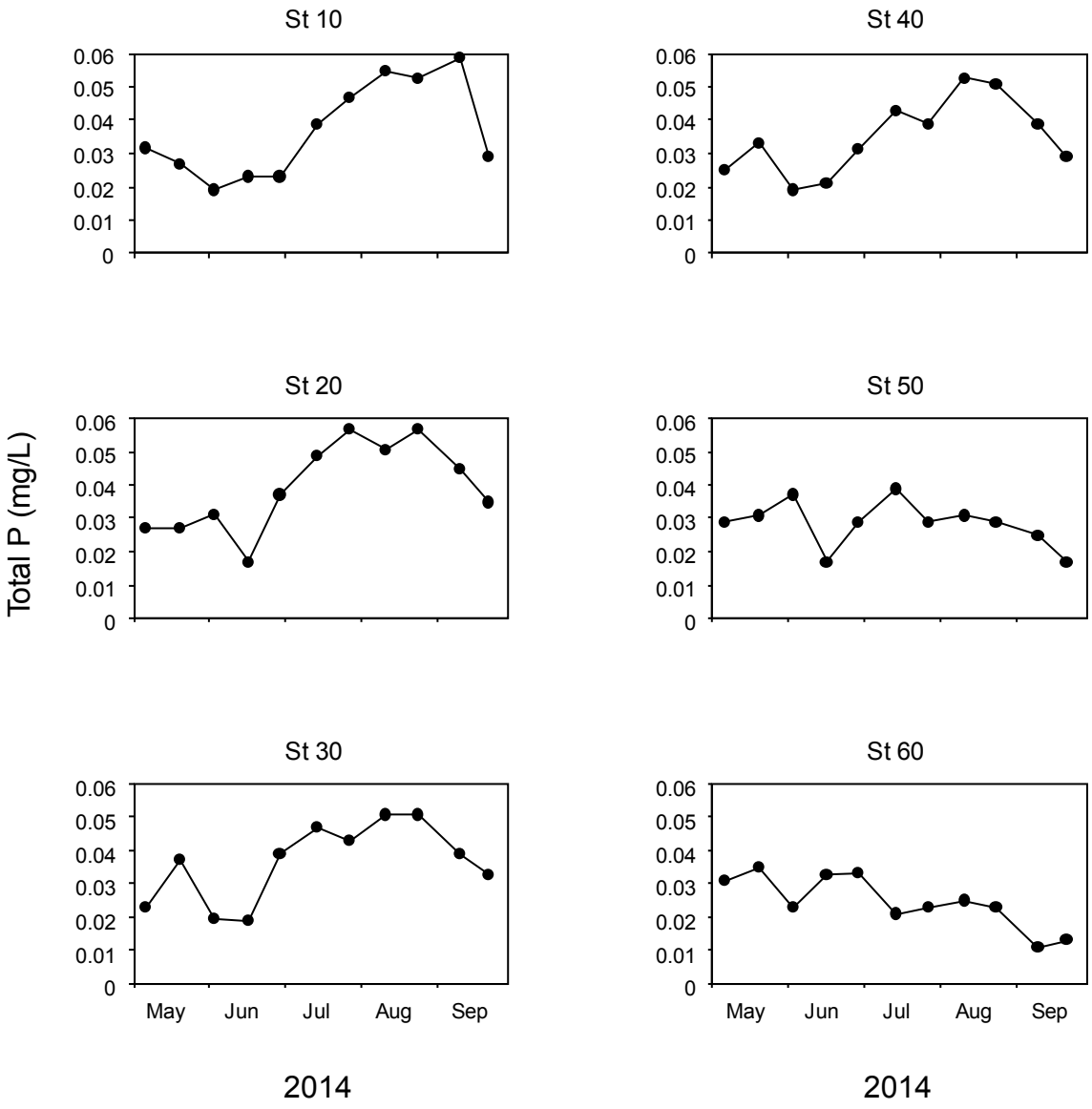

Figure 9. *Seasonal variations in total phosphorus (P) at various stations in Half Moon Lake in 2014.*

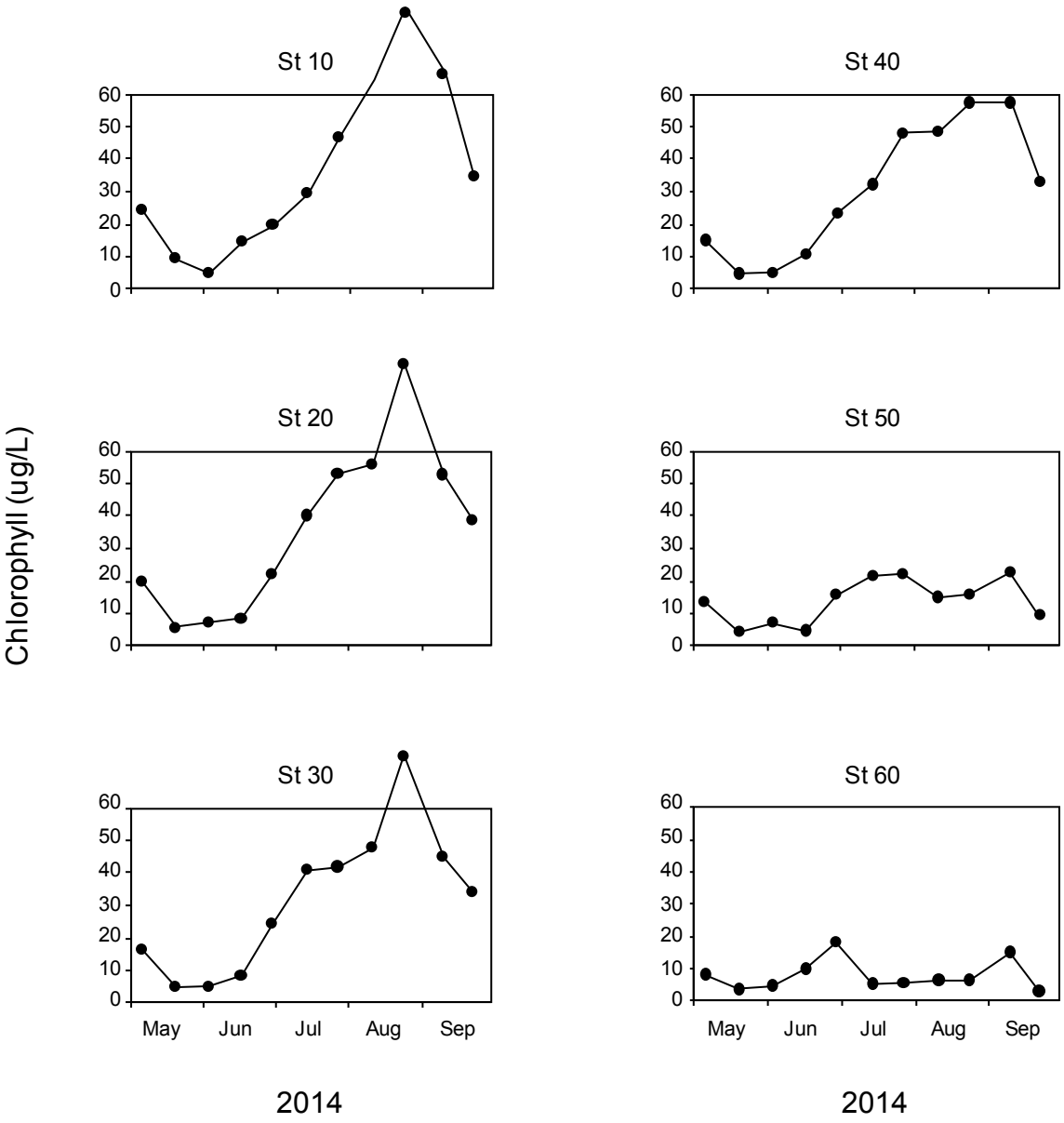

Figure 10. *Seasonal variations in chlorophyll at various stations in Half Moon Lake in 2014.*

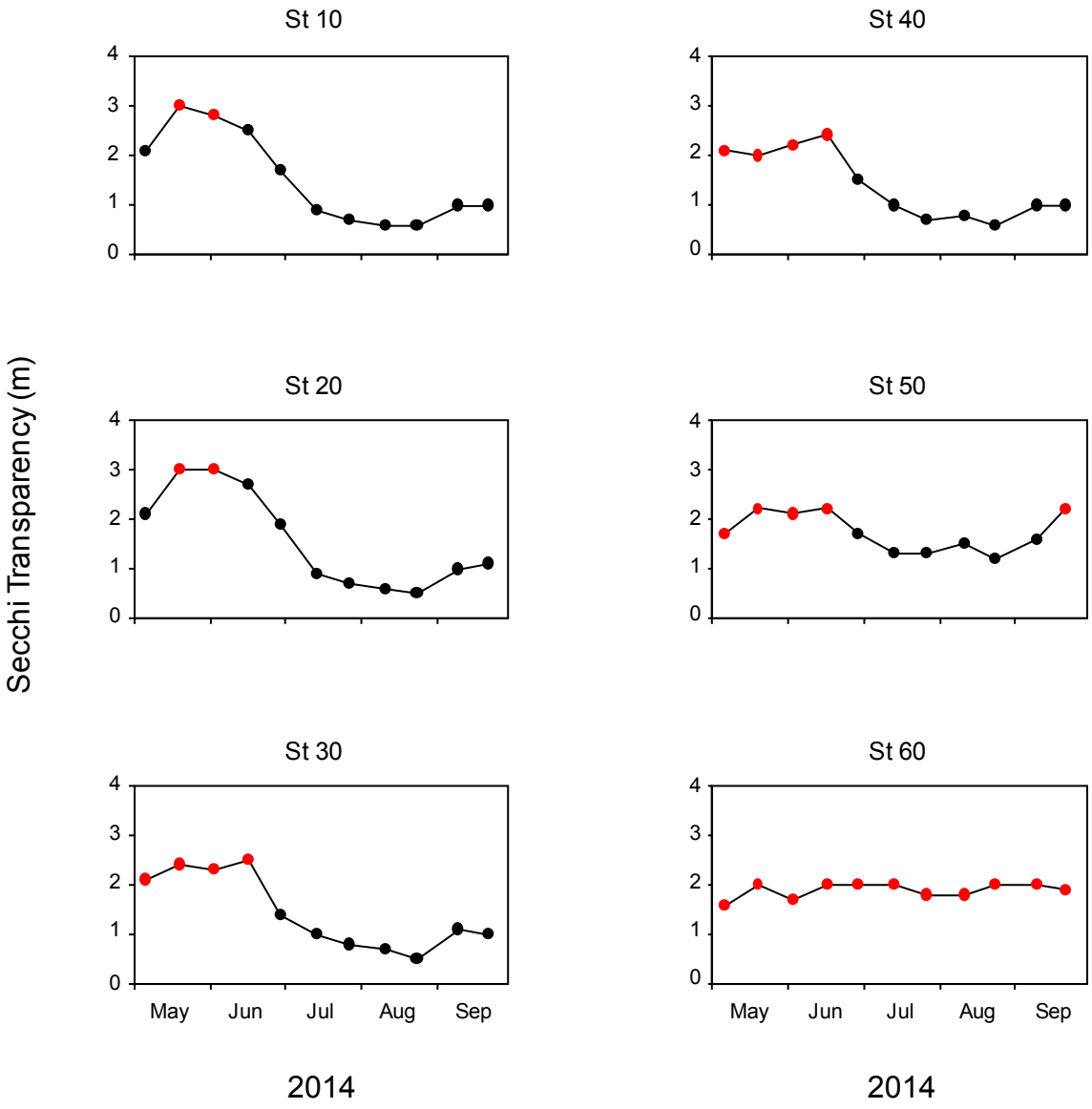

Figure 11. *Seasonal variations in Secchi disk transparency at various stations in Half Moon Lake in 2014. Red circles denote periods when Secchi disk transparency was equivalent to the lake bottom depth.*

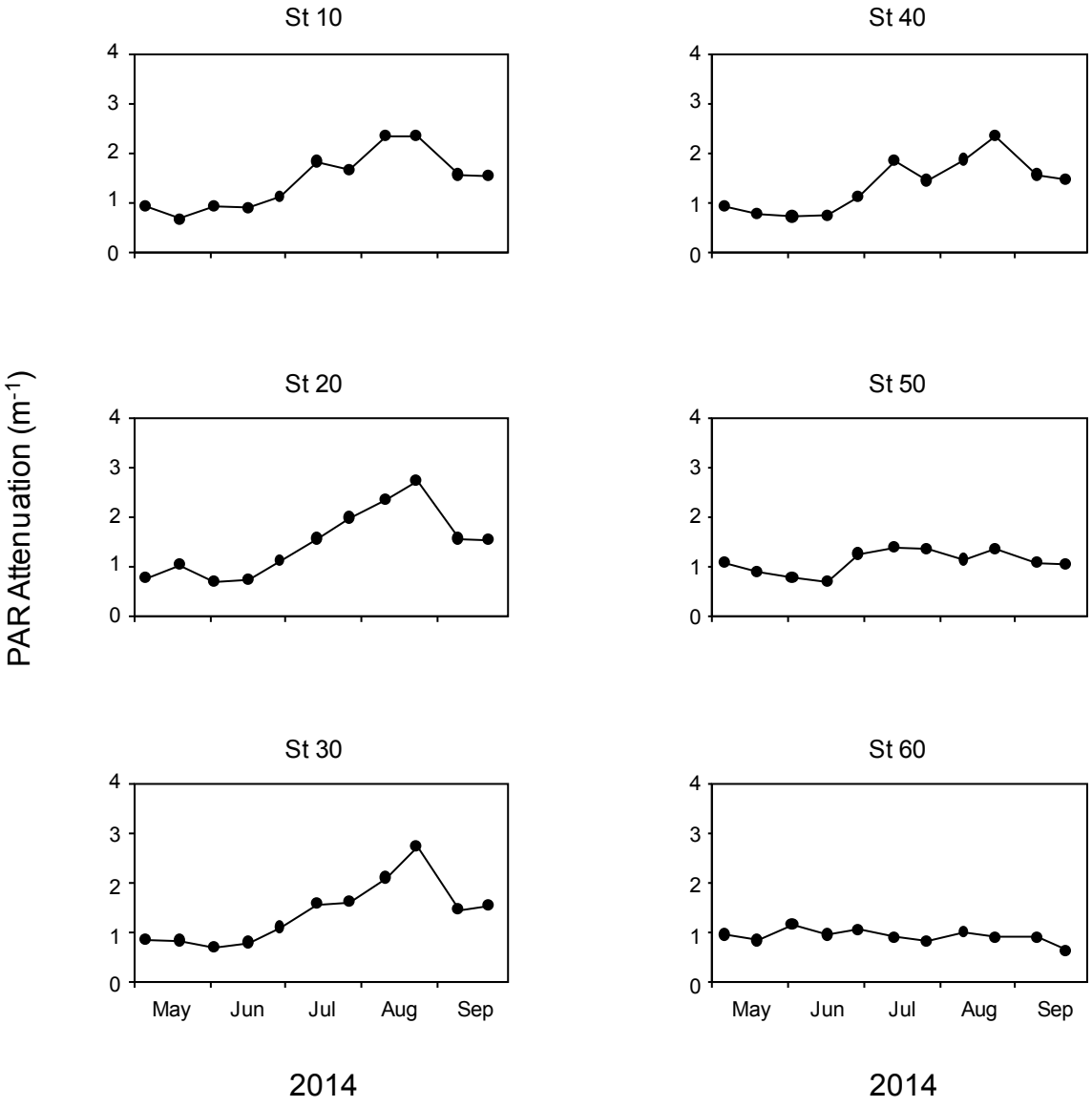

Figure 12. *Seasonal variations photosynthetically-active radiation (PAR) at various stations in Half Moon Lake in 2014.*

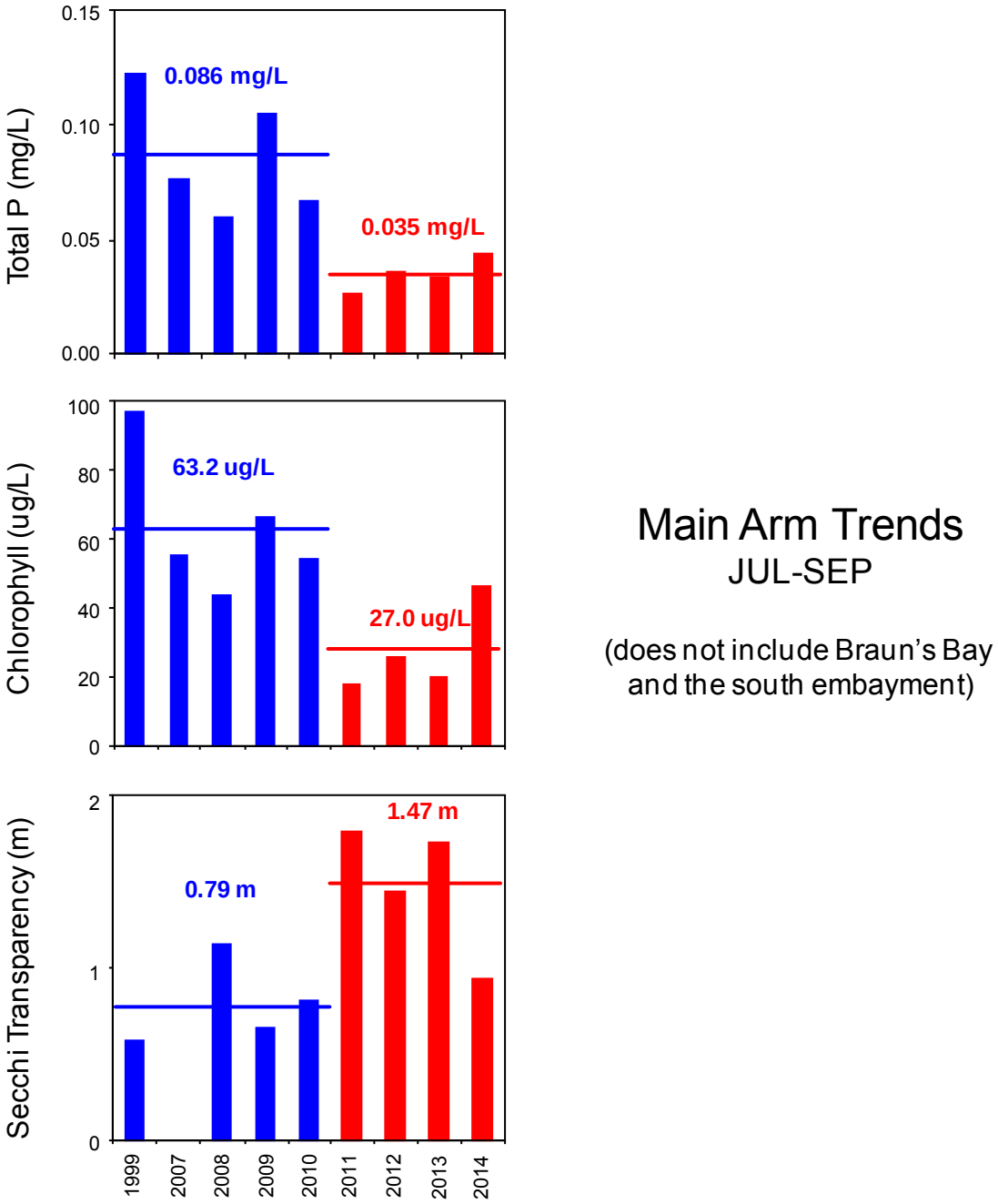

Figure 13. *Summer (JUL-SEP) mean total phosphorus (P), chlorophyll, and Secchi transparency in the main arm (i.e. west and east arms) of Half Moon Lake before (blue bars) and after (red bars) Al treatment (June, 2011). Horizontal lines represent overall pre- and post-treatment means.*

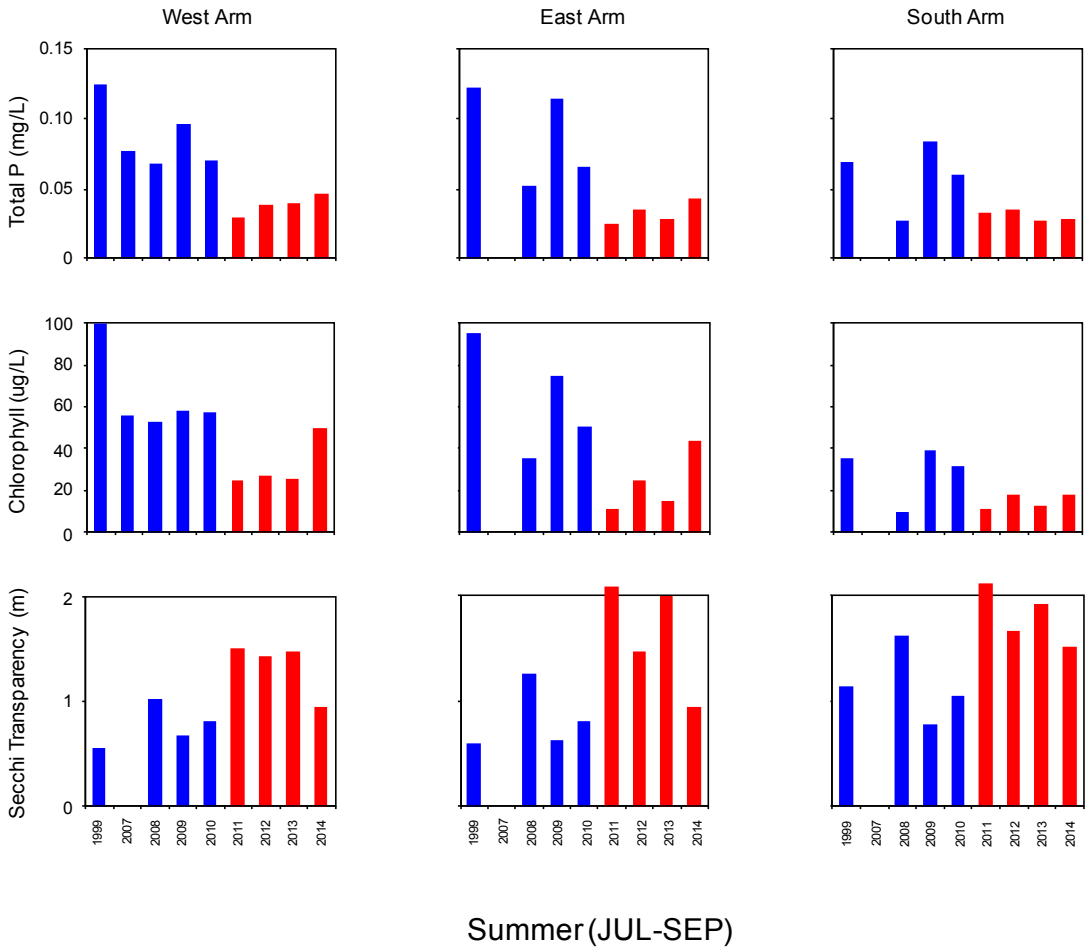

Figure 14. *Summer (JUL-SEP) mean total phosphorus (P), chlorophyll, and Secchi transparency in the west (i.e., station 10 and 20), east (i.e., station 30 and 40), and south (i.e., station 50) arms of Half Moon Lake before (blue bars) and after (red bars) Al treatment (June, 2011).*

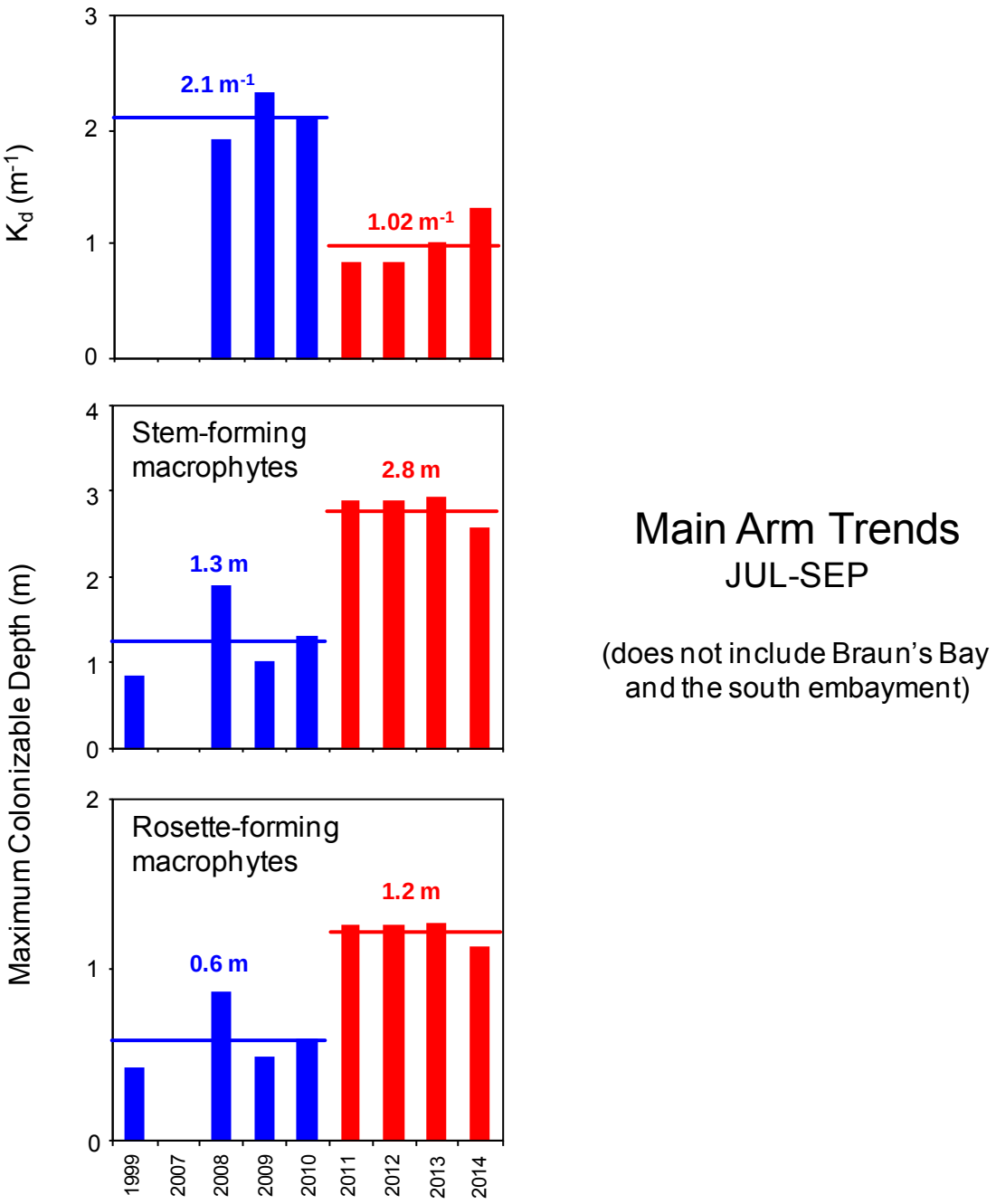

Figure 15. *Summer (JUL-SEP) mean maximum inhabitable depth for stem- and rosette-forming submersed aquatic macrophytes based on Middelboe and Markager (1997) in the main arm (i.e. west and east arms) of Half Moon Lake before (blue bars) and after (red bars) Al treatment (June, 2011). Horizontal lines represent overall pre- and post-treatment means.*

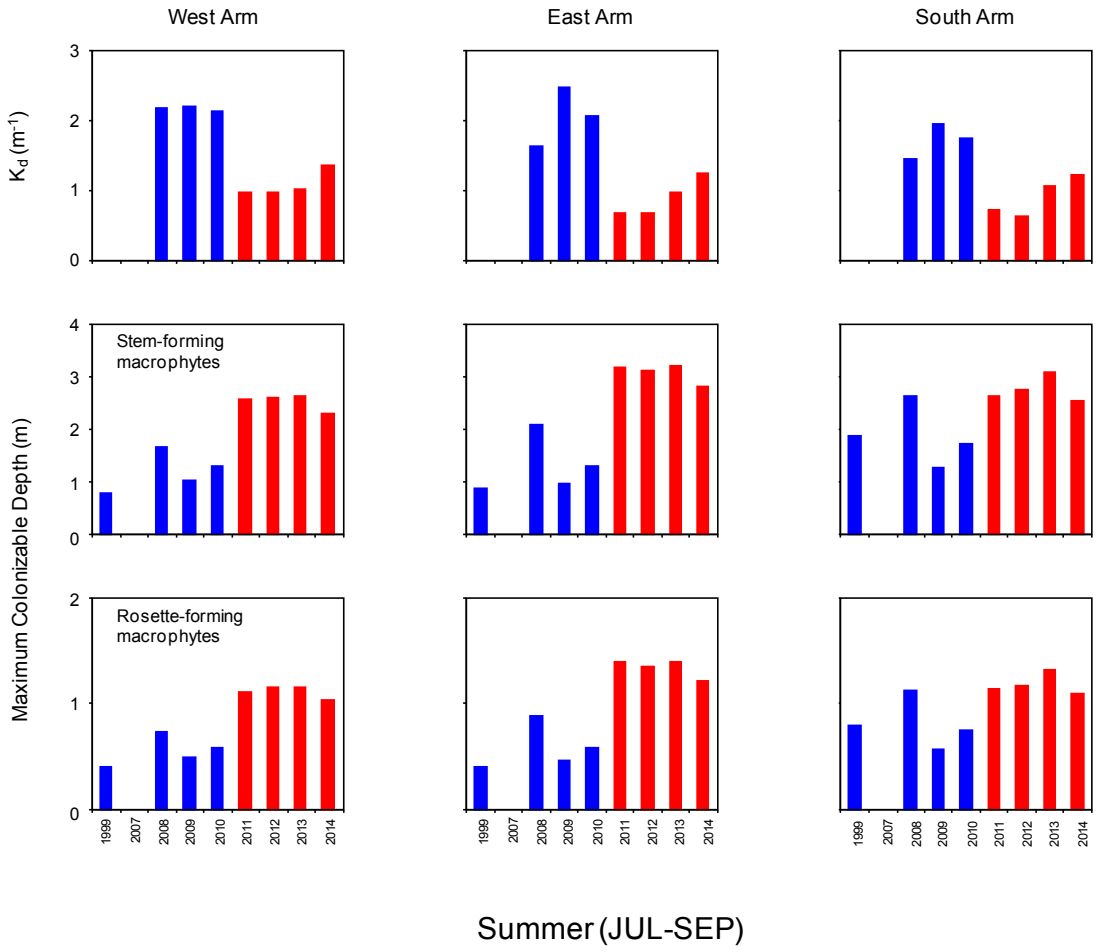

Figure 16. *Summer (JUL-SEP) mean maximum inhabitable depth for stem- and rosette-forming submersed aquatic macrophytes based on Middelboe and Markager (1997) in the west (i.e., station 10 and 20), east (i.e., station 30 and 40), and south (i.e., station 50) arms of Half Moon Lake before (blue bars) and after (red bars) Al treatment (June, 2011). Horizontal lines represent overall pre- and post-treatment means.*

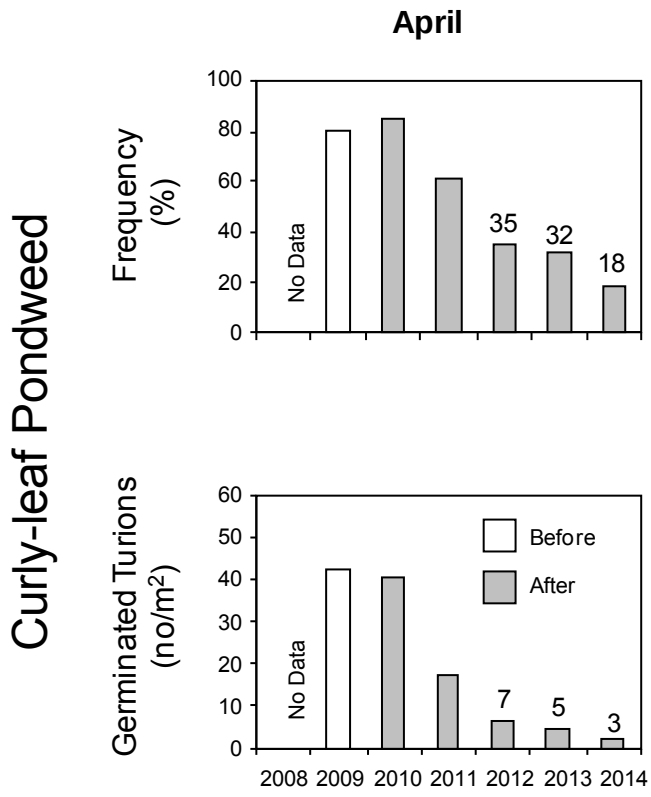

Figure 17. *Percent occurrence (n ~ 140-160; upper panel) and numbers (lower panel) of germinated curly-leaf pondweed tuions in April of various years. White columns represent means before the start of early spring Endothall treatments.*

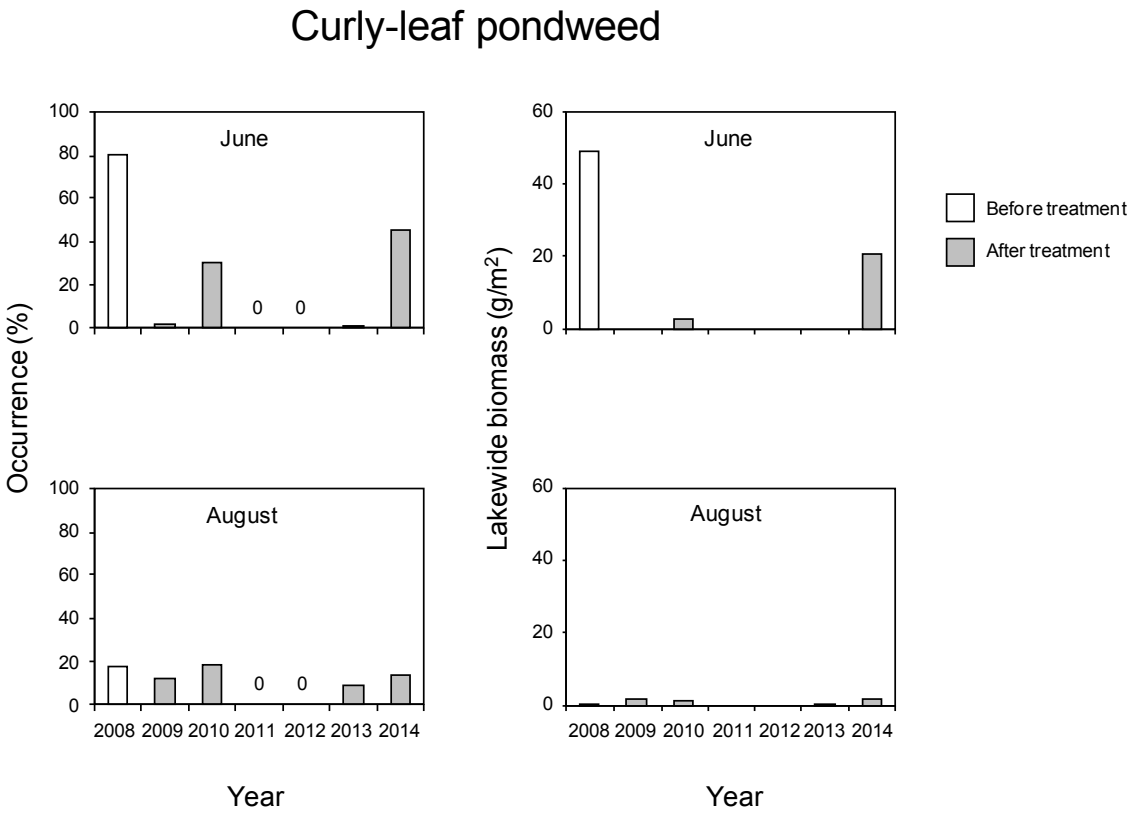

Figure 18. *Curly-leaf pondweed lake-wide mean biomass (n ~ 140-160) in June and August of various years. White columns represent means before the start of early spring Endothall treatments.*

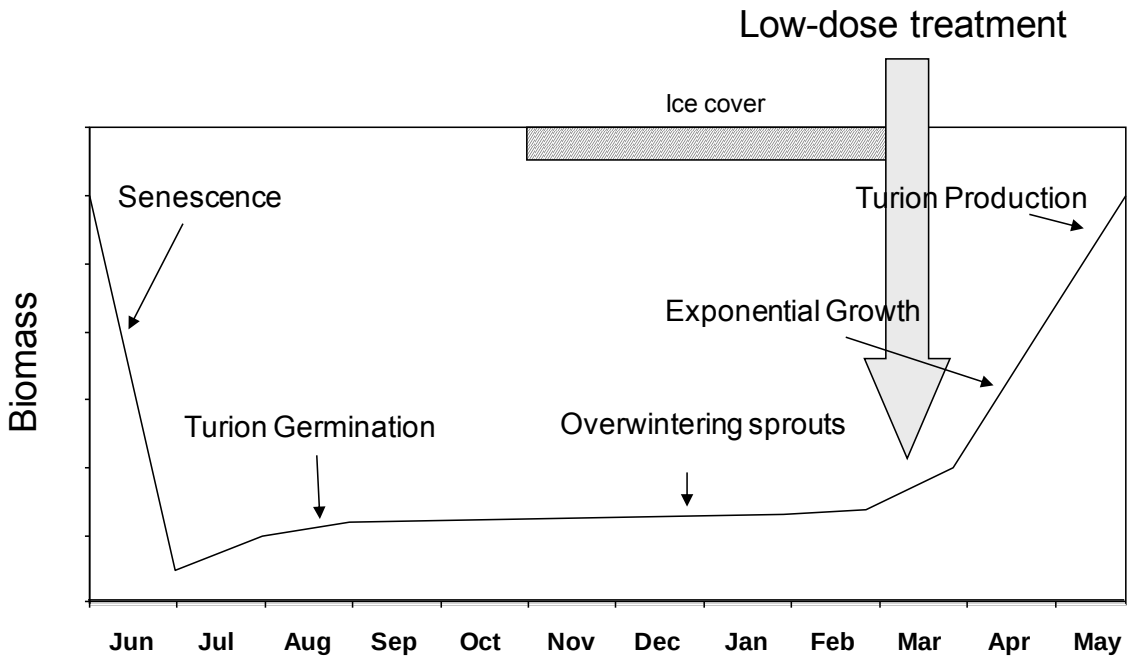

Figure 19. *Conceptual diagram depicting the annual life cycle of curly-leaf pondweed in the upper mid-western United States (Woolf and Madsen 2003).*

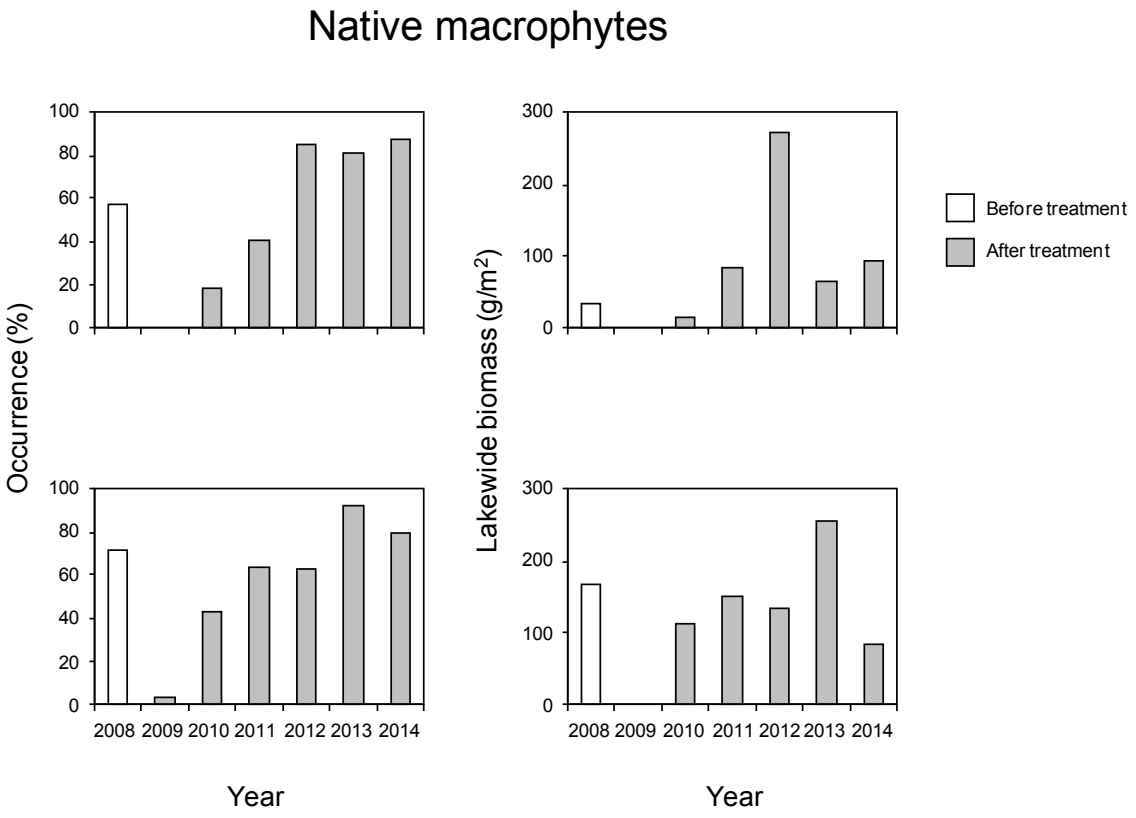

Figure 20. *Native submersed macrophyte lake-wide mean biomass (n ~ 140-160) in June and August of various years. 2008 was the pretreatment year. The pretreatment native macrophyte community in 2008 was dominated by coontail while elodea has dominated the post-treatment assemblage.*

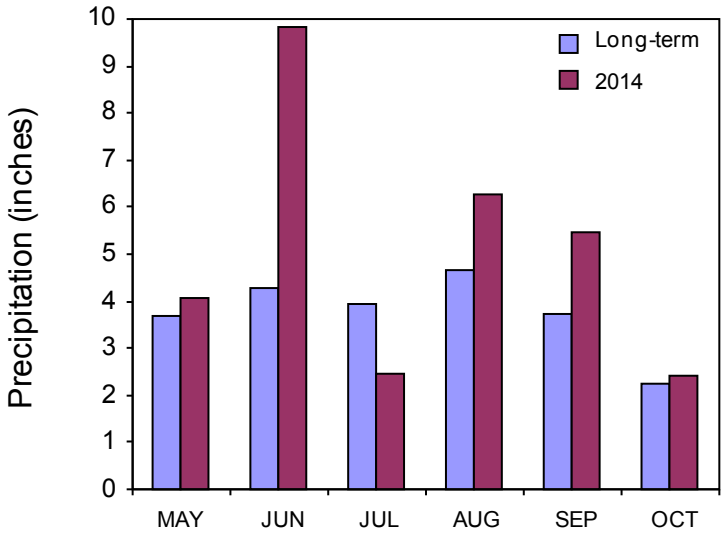

Figure 21. *Mean monthly precipitation measured at the Eau Claire Airport.*

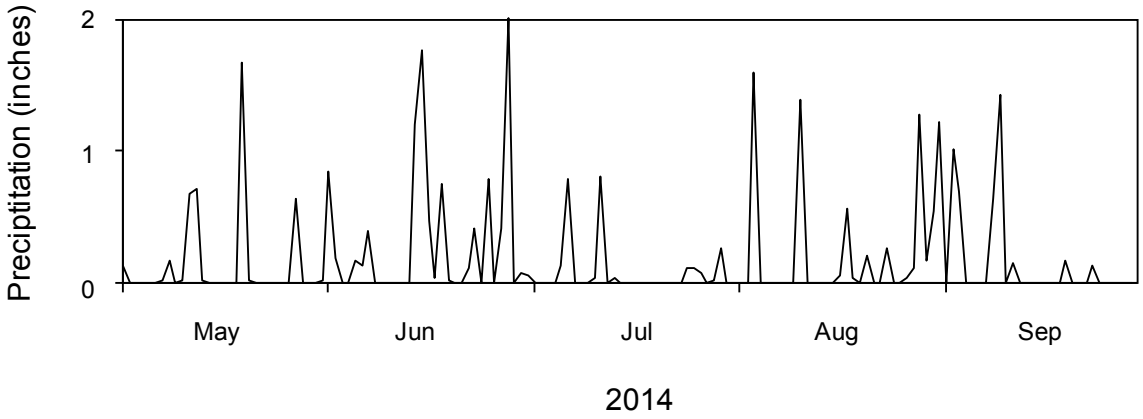

Figure 22. *Variations in daily precipitation in 2014.*

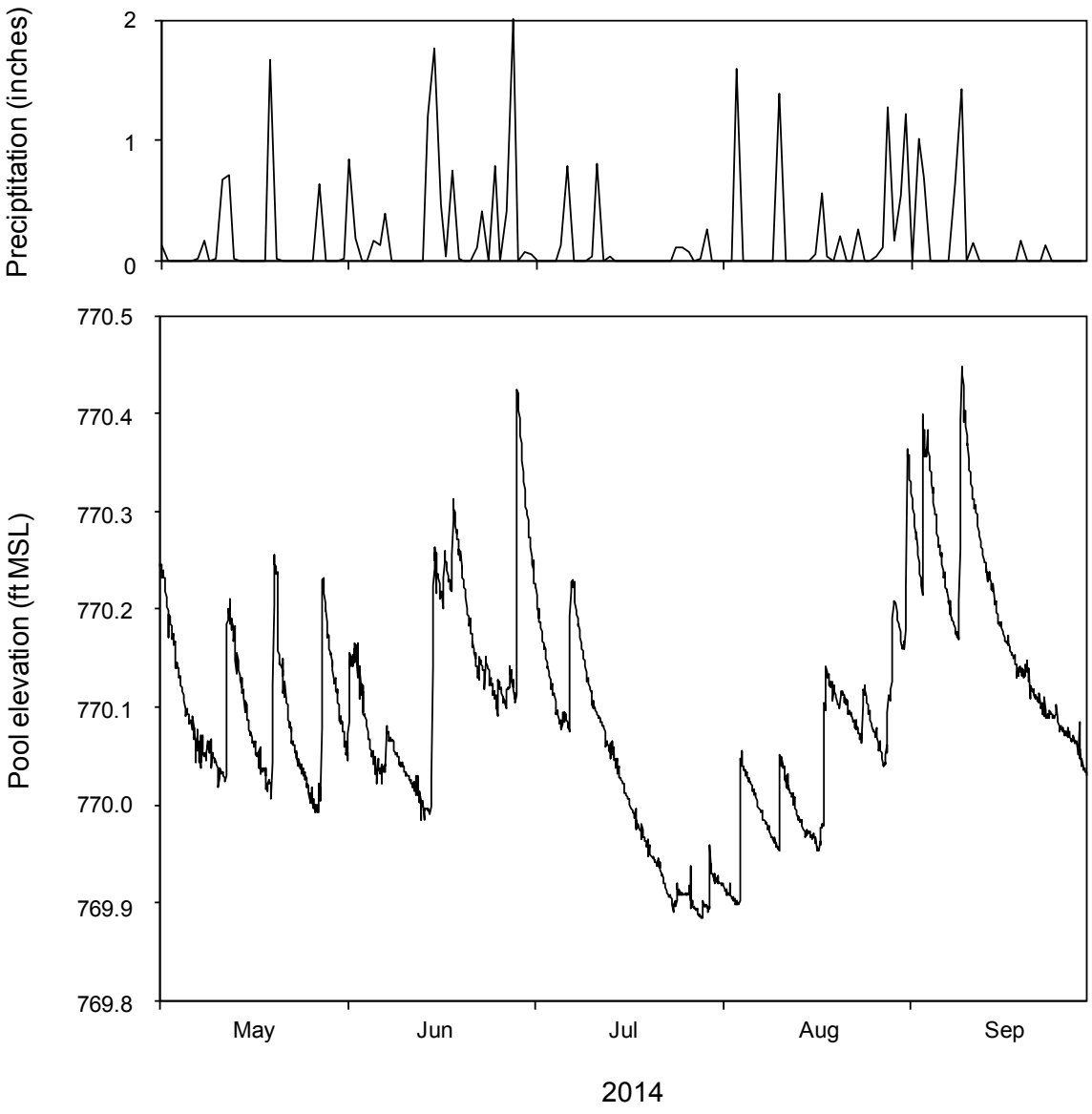

Figure 23. *Variations in pool elevation in 2014.*

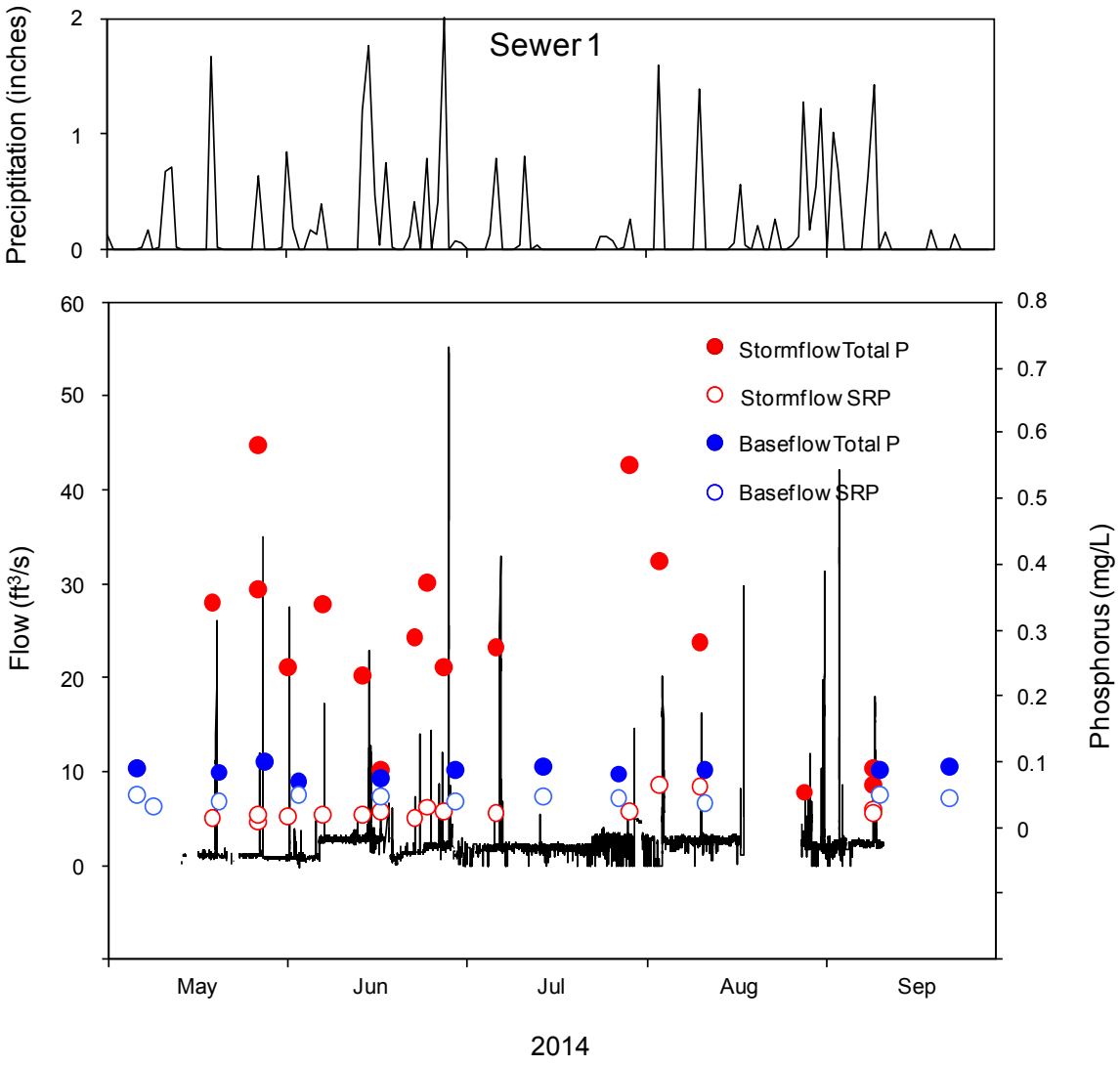

Figure 24. *Variations in flow and phosphorus concentrations for storm sewer 1 in 2014.*

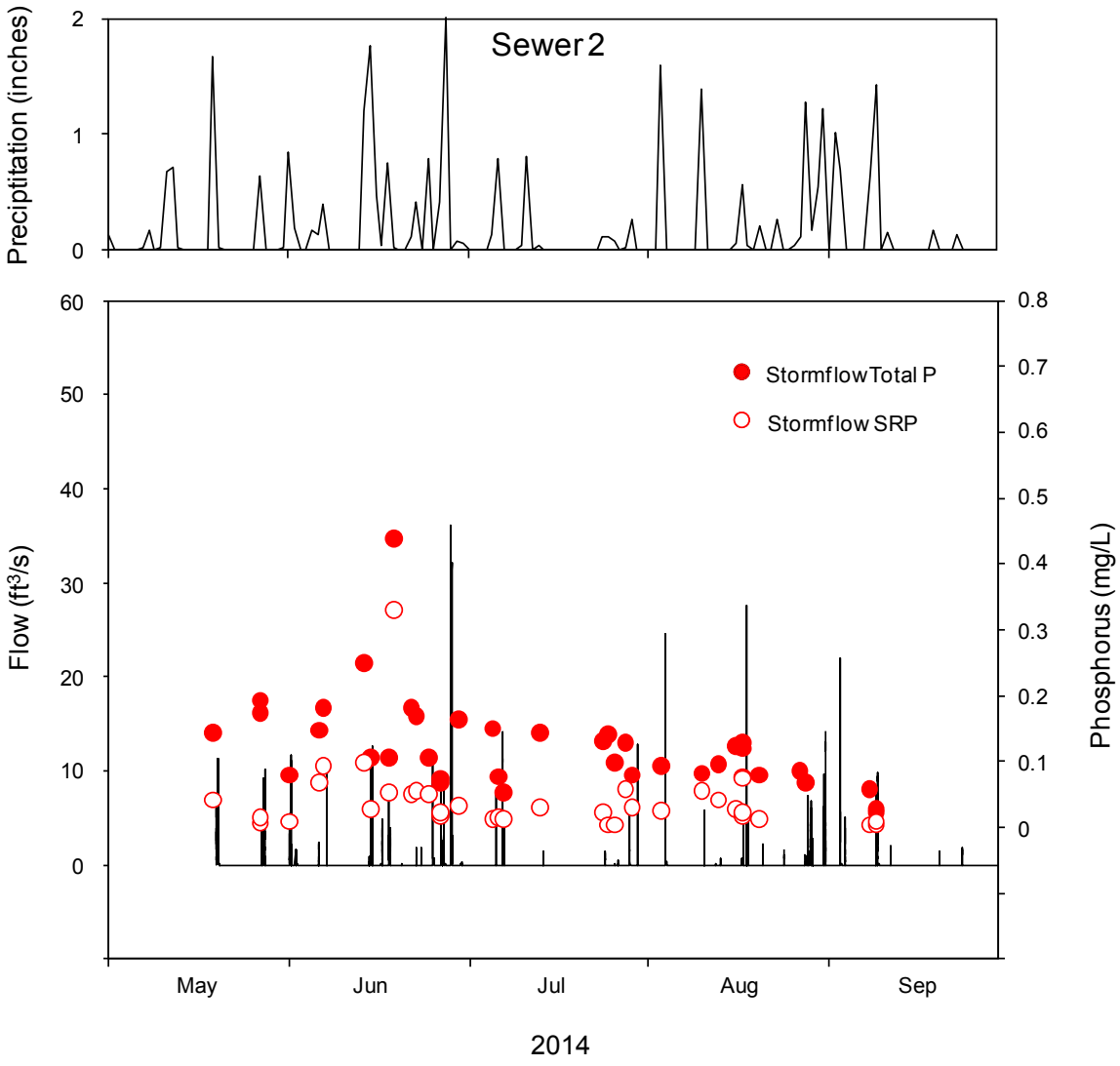

Figure 25. *Variations in flow and phosphorus concentrations for storm sewer 2 in 2014.*

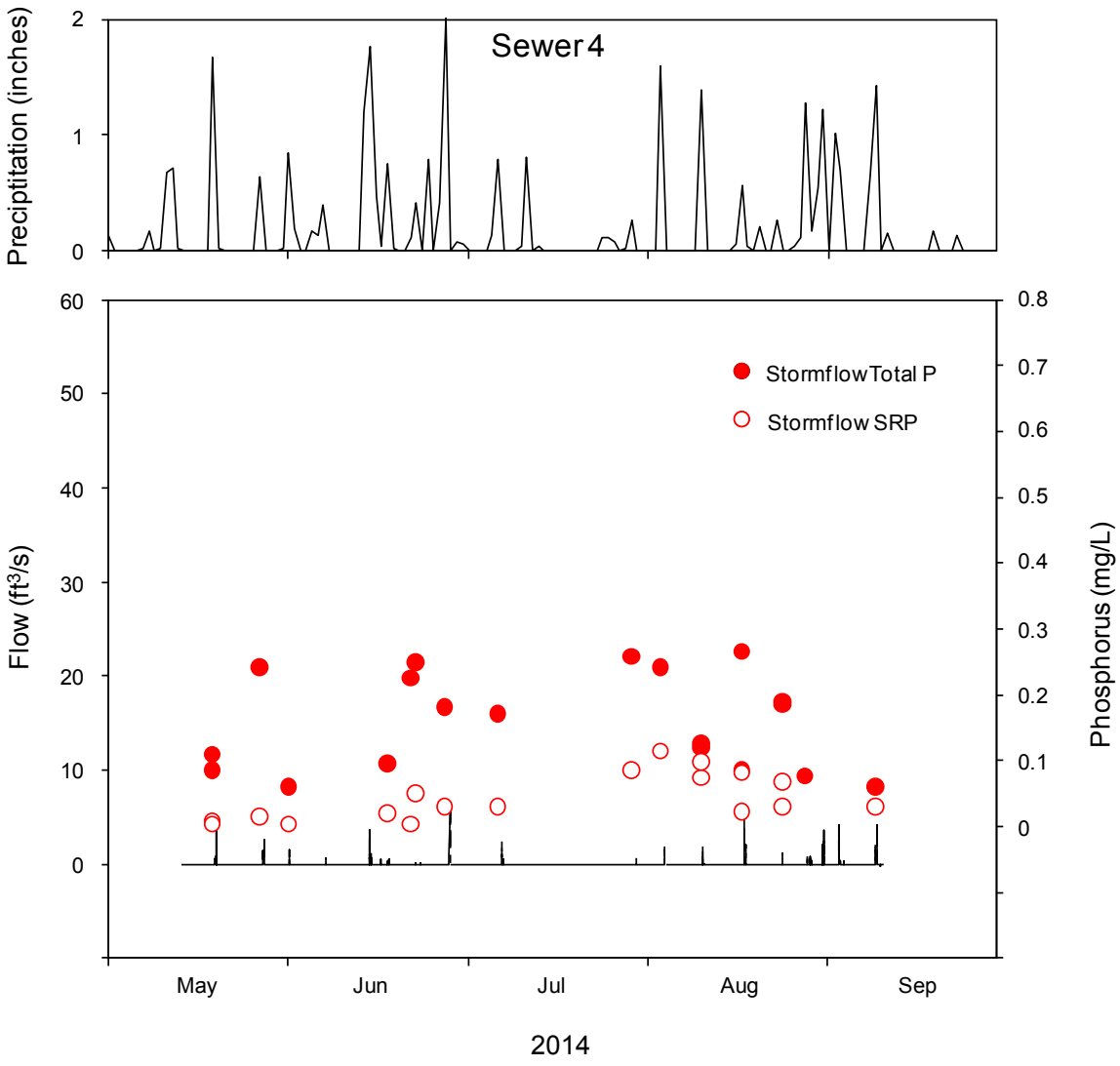

Figure 26. *Variations in flow and phosphorus concentrations for storm sewer 4 in 2014.*

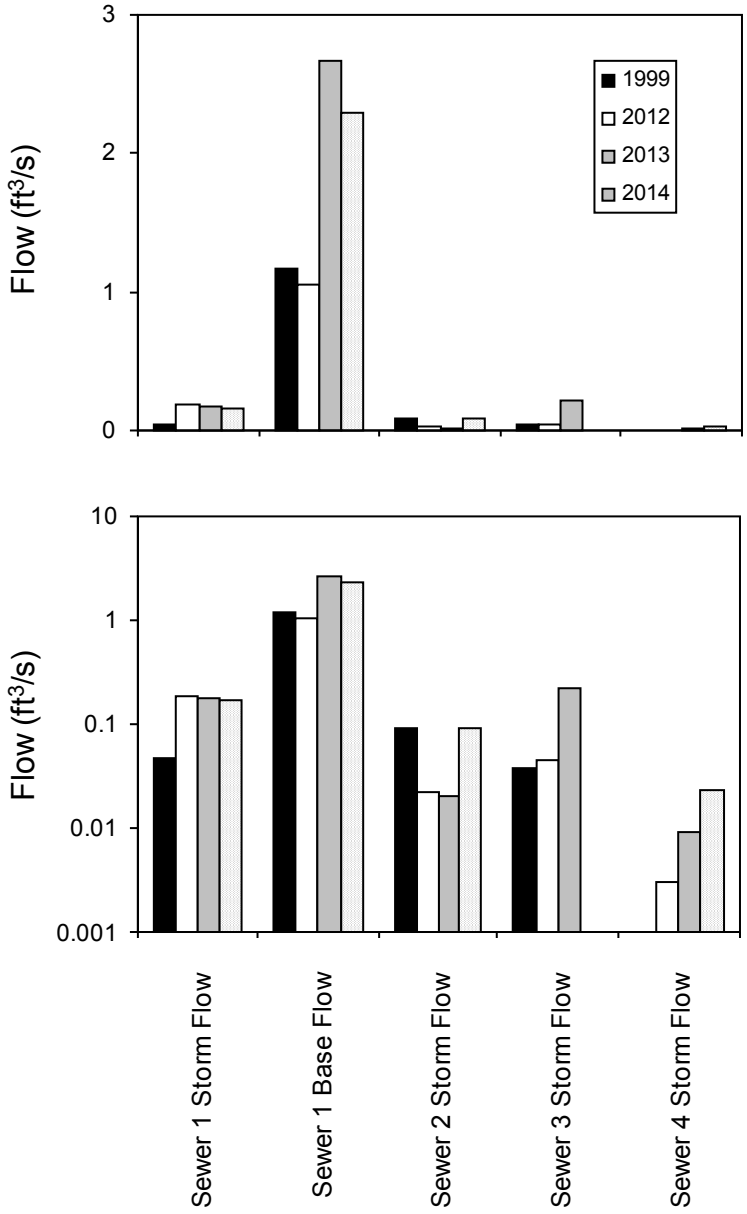

Figure 27. *Comparison of mean summer flow at various storm sewers in 1999 and 2012-14. Please note the log scale in the lower panel.*

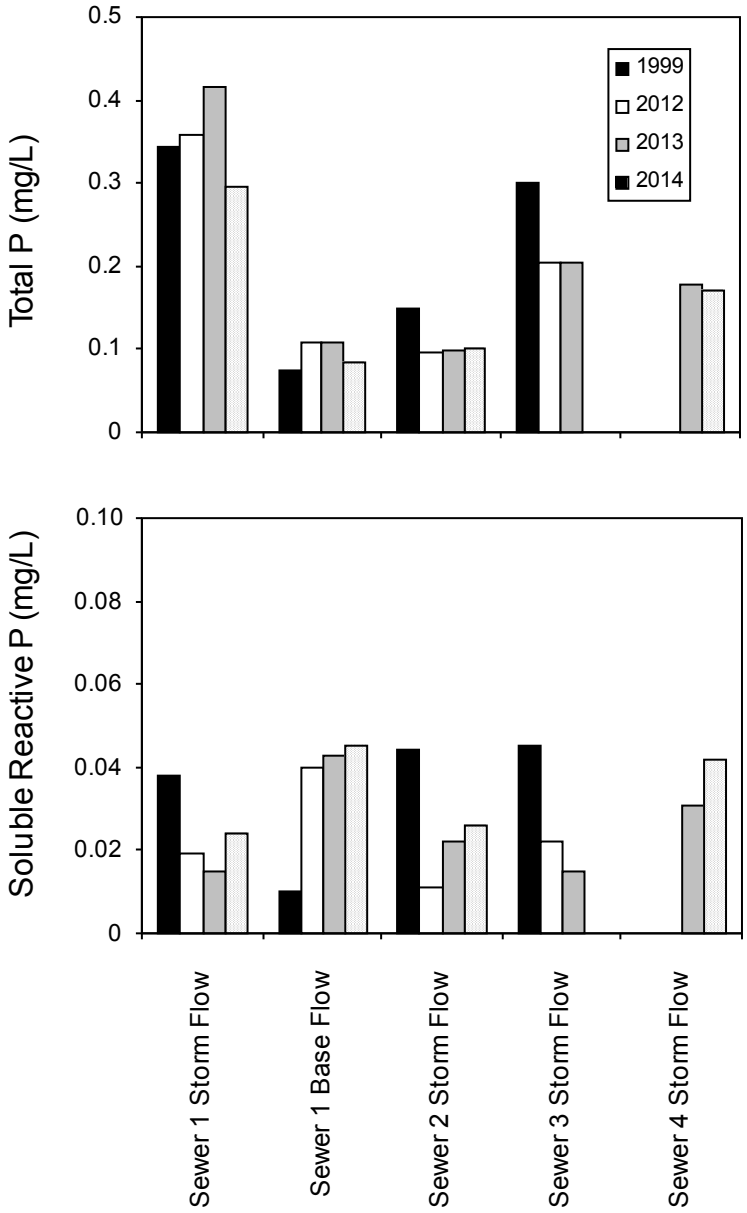

Figure 28. *Comparison of flow-weighted total and soluble reactive phosphorus (P) concentrations at various storm sewers in 1999 and 2012-14.*

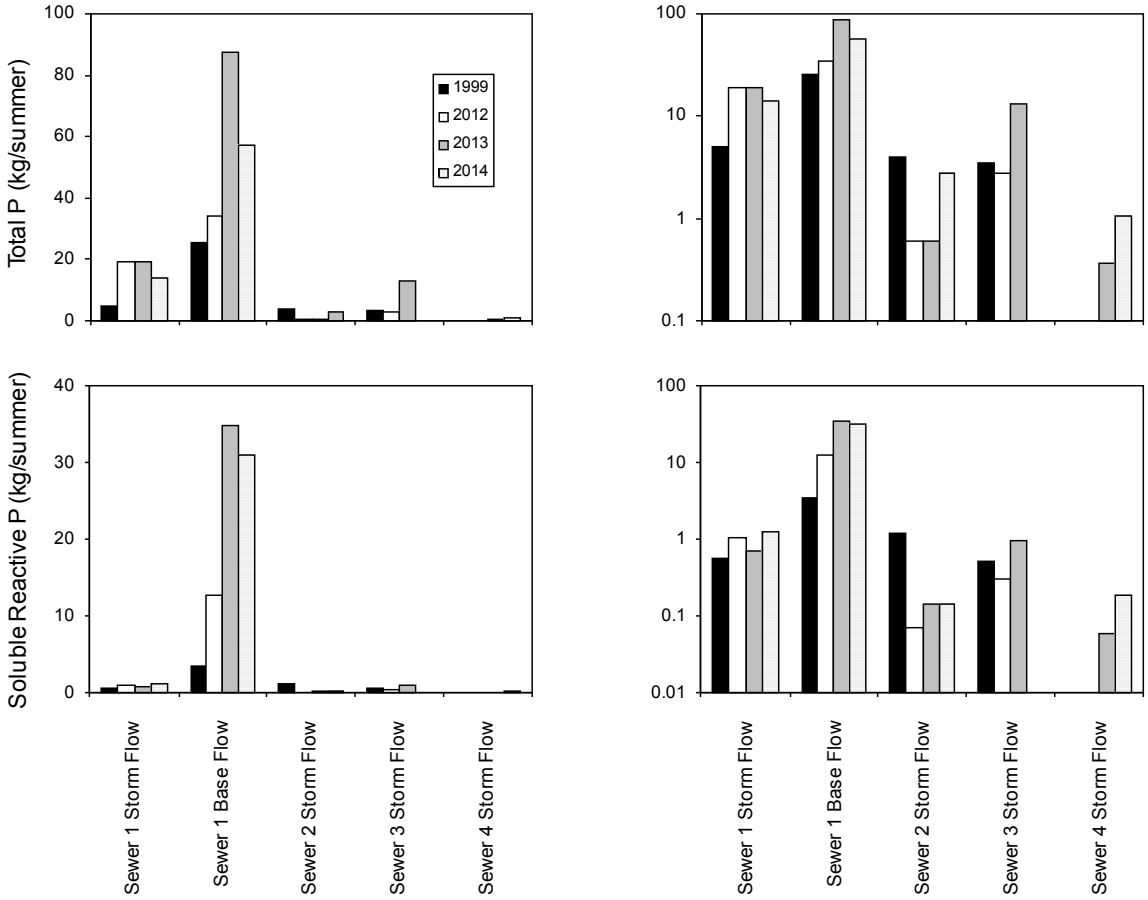

Figure 29. *Comparison of total and soluble reactive phosphorus (P) loading at various storm sewers in 1999 and 2012-14.*

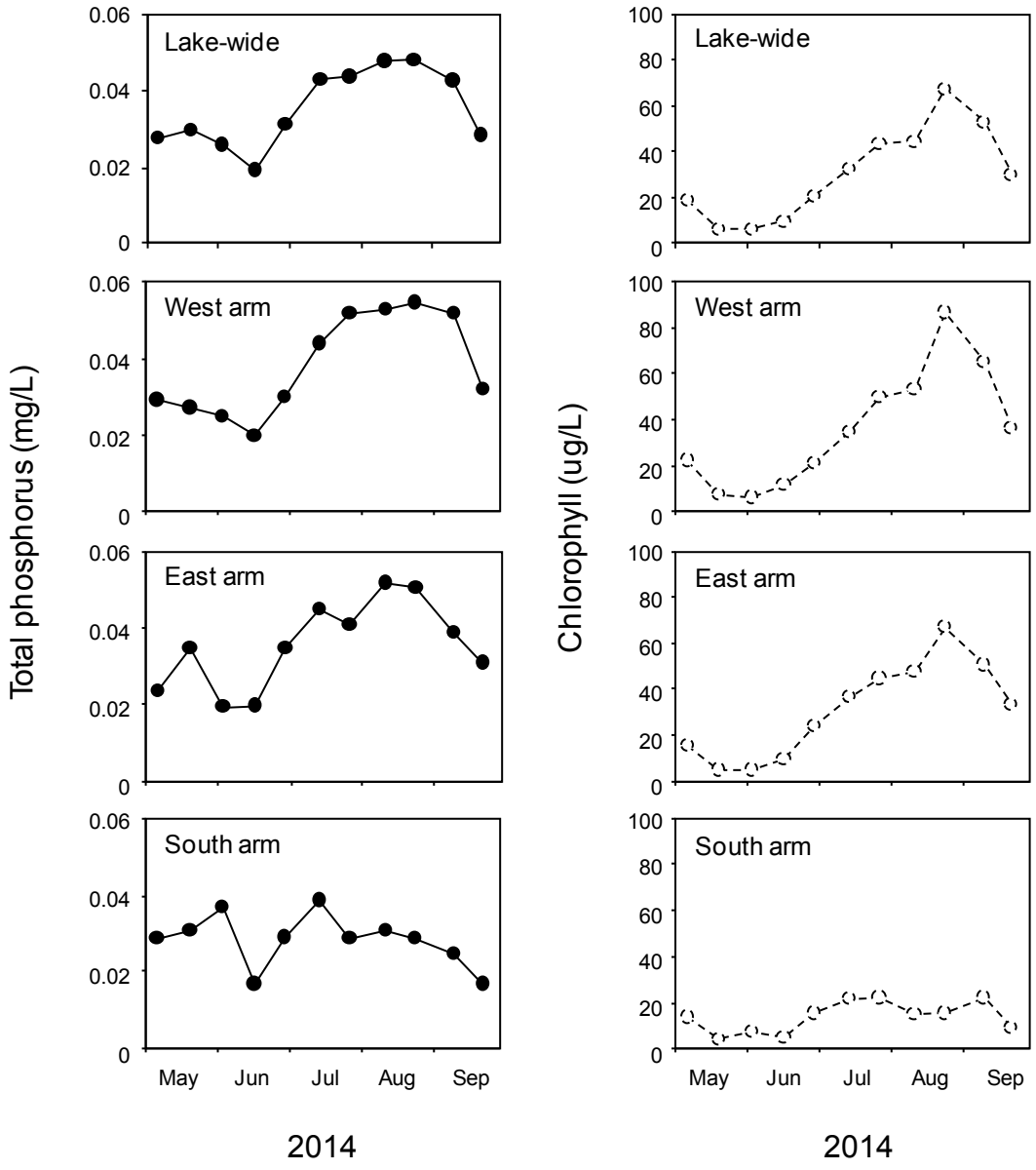

Figure 30. *Seasonal variations in total phosphorus (left panels) and chlorophyll (right panels) concentrations for the lake, west, east, and south arms in 2014.*

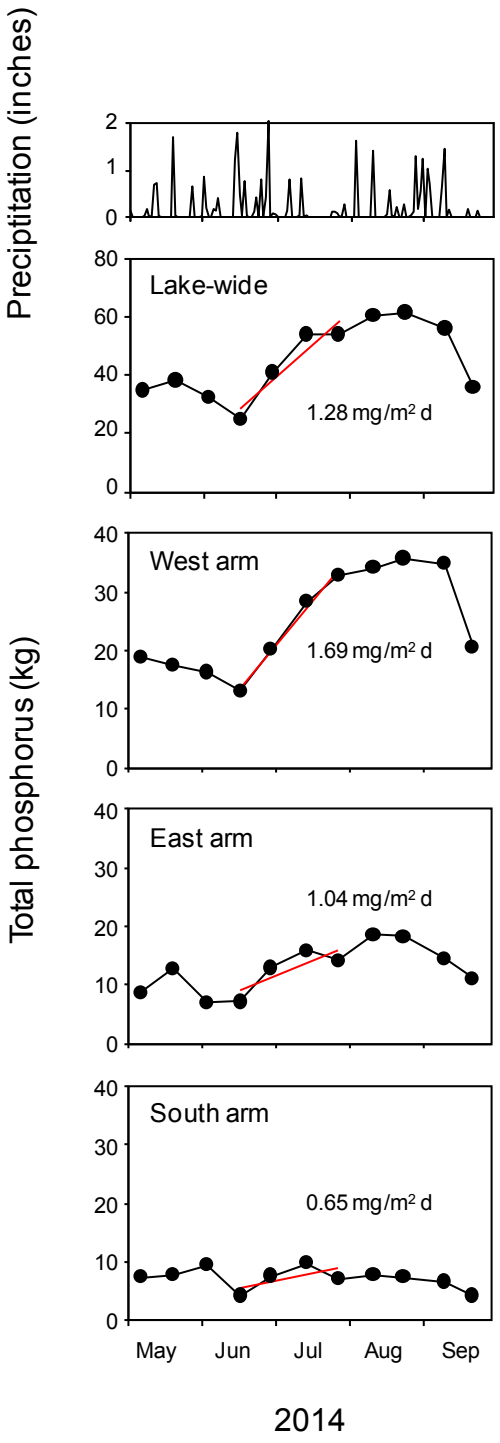

Figure 31. *Seasonal variations in total phosphorus mass for the lake, west, east, and south arms in 2014. Red line denotes the time period (mid-June through late July; 41 day period) used for estimating the net phosphorus mass accumulation rate.*